Title

NDF is a transcription factor that stimulates elongation by RNA polymerase II

Journal

Genes & Development, 36(5-6)

ISSN

0890-9369

Authors

Fei, Jia
Xu, Jun
Li, Ziwei
et al.

Publication Date

2022-03-01

DOI

10.1101/gad.349150.121

Peer reviewed

RESEARCH COMMUNICATION

NDF Is a Transcription Factor that Stimulates Elongation by RNA Polymerase II

Jia Fei,[1] Jun Xu,[2] Ziwei Li,[1] Kevin Xu,[1] Dong Wang,[2] George A. Kassavetis,[3] and James T. Kadonaga[3]

[Key words: Transcription, RNA polymerase II, Elongation, NDF, TFIIS, Gene Expression]

Running Head: NDF Is a Transcription Factor

[1]Department of Molecular Biology and Biochemistry, Rutgers University, Piscataway, New Jersey 08854, USA; [2]Division of Pharmaceutical Sciences, Skaggs School of Pharmacy & Pharmaceutical Sciences, Department of Cellular & Molecular Medicine, School of Medicine, University of California, San Diego, La Jolla, California 92093, USA; [3]Section of Molecular Biology, University of California, San Diego, La Jolla, California 92093, USA

Corresponding authors: jia.fei@rutgers.edu, jkadonaga@ucsd.edu

Abstract

RNA polymerase II (Pol II) elongation is a critical step in gene expression. Here we find that NDF, which was identified as a bilaterian nucleosome-destabilizing factor, is also a Pol II transcription factor that stimulates elongation with plain DNA templates in the absence of nucleosomes. NDF binds directly to Pol II and enhances elongation by a different mechanism than does transcription factor TFIIS. Moreover, yeast Pdp3, which is related to NDF, binds to Pol II and stimulates elongation. Thus, NDF is a Pol II-binding transcription elongation factor that is localized over gene bodies and is conserved from yeast to humans.

In eukaryotic cells, transcription by RNA polymerase II (Pol II) beyond the proximal promoter region is influenced by a number of factors that function by different mechanisms (for reviews, see, for example: Sims et al. 2004; Guo and Price 2013; Chen et al. 2018; Cramer 2019; Conaway and Conaway 2019; Roeder 2019; Lis 2019; Schier and Taatjes 2020). Some factors enable Pol II to overcome nucleosome-mediated inhibition, whereas others interact with Pol II and increase its ability to elongate transcripts. Because of their key role in gene expression, the identification and characterization of the factors that control Pol II elongation is of critical importance.

In our studies of chromatin dynamics, we identified and purified nucleosome-destabilizing factor, NDF, based on its ability to disrupt nucleosomes in a biochemical assay (Fei et al. 2018). We further found that NDF can facilitate Pol II transcription through a downstream nucleosome in vitro and is recruited to thousands of gene bodies upon transcriptional induction in mammalian cells.

NDF is present in most animals but has not been studied in simpler organisms such as yeast. In *Drosophila*, NDF (also known as CG4747) was identified as an MSL (male-specific lethal) complex-interacting protein that targets the complex to active gene bodies and is important for X-chromosome dosage compensation (Wang et al. 2013). In humans, NDF (also known as GLYR1, N-PAC, and NP60) was found as a protein that binds preferentially to H3K36me3 relative to unmethylated H3K36 (Vermeulen et al. 2010). Human NDF was also observed to stimulate H3K4me1 and H3K4me2 demethylation by LSD2/KDM1B (Fang et al. 2013; the region of human NDF that interacts with LSD2/KDM1B is not present in *Drosophila* NDF). NDF has a conserved PWWP motif, which binds to methylated lysines (Qin and Min 2014). In addition, NDF (GLYR1) is present at high levels in all (45/45) tested tissues in humans (Uhlen et al. 2017).

Because NDF was identified as nucleosome-destabilizing factor in biochemical assays with purified nucleosomes (Fei et al. 2018), there was no obvious direct connection between

NDF and Pol II function. However, closer re-examination of our NDF transcription data suggested that purified NDF might enhance transcription by purified Pol II with plain (naked) DNA templates in the absence of nucleosomes. We therefore further investigated the unexpected possibility that NDF stimulates Pol II transcription.

Results & Discussion

NDF stimulates in vitro transcription by Pol II with calf thymus DNA

In initial experiments, we sought to determine whether NDF affects basal transcription by Pol II. To this end, we employed a simple biochemical assay in which transcription by purified Pol II primarily initiates at nicks, gaps, and ends of genomic DNA in a non-sequence-specific manner. This assay was used widely in early transcription studies, such as for the purification of the Pol II elongation factor TFIIS (also known as S-II; see, for example: Sekimizu et al. 1976; Reinberg and Roeder 1987). In our work, we performed reactions with purified yeast Pol II (yPol II) and calf thymus DNA in the absence or presence of NDF and measured the incorporation of radiolabelled CTP into RNA (Supplemental Fig. S1A).

These studies revealed that human NDF (hNDF) as well as *Drosophila* NDF (dNDF) can stimulate non-specific Pol II transcription with plain (naked) DNA. Transcription levels were observed to increase with NDF concentration (with saturation at ~100 nM hNDF and ~200 nM dNDF; Fig. 1AB) as well as to be linear over the first 15 min (Fig. 1CD). As controls, we found that the preparations of hNDF and dNDF did not contain polymerase activity and that the Pol II lacked Pol I and Pol III activity (Supplemental Fig. S1B). In addition, these experiments were performed at a Pol II concentration in the linear concentration-activity range (Supplemental Fig. S1C).

Yeast Pdp3 protein is related to NDF and stimulates transcription

The ability of both dNDF and hNDF to stimulate transcription by yeast Pol II suggested that there might be NDF-related factors in yeast. We investigated this possibility and identified *Saccharomyces cerevisiae* Pdp3 (yPdp3) as being closely related to hNDF (Supplemental Fig. S2). yPdp3 is a PWWP domain-containing protein (Gilbert et al. 2014) with extensive sequence similarity (~25% identity; ~39% similarity) to the N-terminal region of hNDF. yPdp3 lacks the catalytically-inactive dehydrogenase domain at the C-terminus of hNDF. Notably, the similarity between yPdp3 and hNDF extends throughout the entire yPdp3 protein and is not restricted to the PWWP domain. Moreover, like bilaterian NDF, yPdp3 is localized over gene bodies (Flury et al. 2017).

To test the biochemical activities of yPdp3, we purified the protein (Supplemental Fig. S3A) and found that it is able to stimulate in vitro transcription by yPol II with the calf thymus DNA assay (Supplemental Figs. S3B, S3C). In addition, yPdp3 did not exhibit synergism with hNDF in the stimulation of transcription (Supplemental Fig. S3D). This finding is consistent with yPdp3 and hNDF activating transcription by a similar mechanism. Hence, yPdp3 is related to NDF and also stimulates transcription by Pol II.

hNDF and yPdp3 bind directly to Pol II

Because NDF and yPdp3 stimulate Pol II transcription, we tested their ability to interact with Pol II. First, in HeLa cells that stably express FLAG-hNDF-GFP, we found that the hNDF fusion protein co-immunoprecipitates with the endogenous Pol II (Fig. 1E). Second, in wild-type HeLa cells, we saw that the endogenous hNDF co-immunoprecipitates with the endogenous Pol II (Fig. 1F). Third, we carried out sucrose gradient sedimentation analyses with purified yeast Pol II and purified hNDF, and observed that Pol II binds directly to NDF (Supplemental Fig. S4). Fourth, we observed that purified hNDF interacts with purified hPol II (Supplemental Fig. S5A). Fifth, we found that purified yPdp3 associates with purified yPol II (Supplemental Fig. S5B). Consistent with this finding, it was observed that the isolation of TAP-tagged yPdp3 from yeast

extracts resulted in the copurification of the Rpb2 and Rpb4 subunits of yeast Pol II (Gilbert et al. 2014). These results collectively indicate that hNDF as well as yPdp3 bind directly to Pol II.

NDF as well as Pdp3 can stimulate transcription elongation by Pol II

Next, we more rigorously investigated the effect of hNDF upon Pol II transcription with well-defined DNA templates. Because NDF is localized over the transcribed regions of active genes in *Drosophila* (Wang et al. 2013) and in humans (Vermeulen et al. 2010; Fei et al. 2018), we tested whether hNDF affects transcriptional elongation with purified human Pol II (hPol II).

In these experiments, we assembled Pol II elongation complexes with hPol II and examined the effect of hNDF on elongation through two different downstream sequences. To this end, we assembled functional transcription elongation complexes by using the method that was developed by Kashlev and colleagues (Sidorenkov et al. 1998; Kireeva et al. 2000; Komissarova et al. 2003). First, we hybridized a short 5'-labeled primer RNA to the template DNA strand, and then added purified hPol II to reconstitute the catalytically active elongation complex. Next, we annealed a 5'-biotinylated non-template DNA strand to give the elongation complex, as shown in upper left diagram in Fig. 2A. We then ligated different downstream sequences to the complex and analyzed the ability of hNDF to stimulate hPol II elongation through these sequences (Fig. 2A).

With the *Xenopus borealis* 5S rDNA as the downstream sequence, we found that hNDF enhances the formation of full-length run-off transcripts (Fig. 2B). Hence, beginning with a productive hPol II elongation complex, hNDF is able to stimulate the elongation of Pol II in the production of full-length run-off transcripts.

We additionally tested transcription into the ~400 GAA triplet repeats in the human *FXN* gene. The expanded GAA triplets in the first intron of the *FXN* gene impede Pol II elongation and thus appear to cause Friedreich's ataxia, which is caused by a deficiency in the levels of the FXN protein (Bidichandani et al. 1998; Punga and Bühler 2010; Li et al. 2015). Transcription into the downstream *FXN* sequences showed that hNDF substantially increases the amount of

elongation of hPol II into the GAA triplet repeats (Fig. 2C). We also found that yPdp3 stimulates transcription elongation into downstream *FXN* sequences with GAA repeats (Supplemental Fig. S6).

These findings indicate that NDF as well as Pdp3 can stimulate the elongation of transcription by Pol II with defined DNA templates. NDF was identified based on its ability to destabilize nucleosomes, and it was found to be able to facilitate Pol II transcription through a nucleosome (Fei et al. 2018). Here, we show that hNDF as well as the related yPdp3 protein can stimulate Pol II elongation with plain (naked) DNA in the absence of nucleosomes (Figs. 1 and 2). Thus, the enhancement of Pol II elongation by NDF/Pdp3 occurs independently of nucleosome-mediated inhibition of transcription.

NDF enhances Pol II elongation by a different mechanism than does TFIIS

We then examined whether or not the transcript-elongating function of NDF is similar to that of TFIIS (also known as S-II), which rescues arrested and backtracked Pol II elongation complexes by stimulating the polymerase-mediated cleavage of the 3' end of the nascent transcript (for reviews, see: Wind and Reines 2000; Sims et al. 2004; Nudler 2012; Guo and Price 2013; Cramer 2019; Conaway and Conaway 2019; Schier and Taatjes 2020). The TFIIS-stimulated transcript cleavage enables backtracked Pol II to be properly aligned with the 3' end of the transcript so that the polymerase can resume transcription elongation.

To test the ability of NDF to rescue arrested Pol II, we performed Pol II elongation assays with a downstream 9A pause site that strongly arrests Pol II elongation (Sigurdsson et al. 2010) (Fig. 3A). Unlike TFIIS (Sigurdsson et al. 2010), NDF has only a slight effect upon the transcription of Pol II through the 9A pause site (Fig. 3B). To investigate whether NDF can rescue backtracked/arrested Pol II and resume elongation, we added NDF to pre-formed backtracked/arrested Pol II complexes and chased with rNTPs (Fig. 3C). We found that NDF, in contrast to TFIIS, is not able to rescue purified arrested Pol II elongation complexes. We further observed that NDF, unlike TFIIS, is not able to stimulate the cleavage of the nascent transcripts

by stalled and backtracked Pol II (Fig. 3D). These findings indicate that NDF and TFIIS stimulate Pol II elongation by different mechanisms. This conclusion is also supported by the observation that there is synergy between TFIIS and NDF in the stimulation of Pol II transcription with the calf thymus DNA template system (Supplementary Fig. S7).

NDF has a small but distinct effect upon ongoing transcription in cells

Because NDF functions as a Pol II elongation factor in biochemical assays, we investigated whether it participates in ongoing transcription in cells. Although there are other Pol II elongation factors that could potentially compensate for the loss of NDF, we nevertheless felt that it would be useful to examine whether NDF contributes to transcription in cells. Also, in previous work, we found that the loss of NDF results in a decrease in steady-state transcripts by RNA-seq as well as a decrease in run-on transcription in nuclei by GRO-seq (Fei et al. 2018). To assess whether NDF has an effect upon ongoing transcription in cells, we used the Bru-seq method (Paulsen et al. 2013). This technique involves the transient treatment of cells with 5-bromouridine, which is a relatively non-toxic uridine analog that is incorporated into nascent transcripts.

We therefore performed Bru-seq with wild-type (WT) and NDF knockout (KO) HeLa cells. These experiments showed that genes with high NDF occupancy levels generally exhibit a small but distinct decrease in ongoing transcription in the KO cells relative to the WT cells (Fig. 4A; Supplemental Fig. S8A). We displayed the genes in four clusters, which are defined in the figure legend. Notably, Cluster 1 contains genes with strong signals for RNA-seq, NDF ChIP-seq, and H3K36me3 ChIP-seq in WT HeLa cells. We did not observe a distinct correlation between the Bru-seq NDF KO/WT ratio and RNA-seq signal strength (Fig. 4B; Supplemental Fig. S8B). Hence, the Bru-seq data suggest that NDF contributes to ongoing transcription in cells, such as in the cluster 1 genes with high NDF occupancy levels. The loss of NDF does not, however, result in a strong decrease of transcription in cells. In addition, the observed effects could be due to the function of NDF in Pol II stimulation and/or nucleosome disruption.

We further tested the effect of the loss of NDF upon ongoing transcription by carrying out Bru-seq analyses in human SW480 cells (Supplemental Fig. S9). As in HeLa cells, we observed that the loss of NDF in SW480 cells results in a small but distinct decrease in transcription at genes that are associated with high levels of NDF (Supplemental Fig. S9B). To determine whether the decrease in transcriptional activity was due to the loss of NDF, we expressed recombinant NDF in the NDF knockout (KO) cells to give KO+NDF rescue cells (Supplemental Fig. S9A). We then carried out Bru-seq analyses of the KO+NDF rescue cells versus wild-type cells, and observed that the expression of NDF in the KO cells resulted in the restoration of the loss in transcription at the high NDF genes (Supplemental Fig. S9C). These data support the conclusion that NDF contributes to ongoing transcription at NDF-associated genes in human cells.

Because there are many different factors that participate in the Pol II elongation process, it is likely that the small effect observed upon loss of NDF is due to compensation by the other Pol II elongation factors. In this regard, it is relevant to note that modest effects upon transcription have been observed upon loss or inhibition of other Pol II elongation factors such as TFIIS, Elongin, and ELL (see, for example: Sheridan et al. 2019; Ardehali et al. 2021; Wang et al. 2021; Gopalan et al. 2018).

NDF is a Pol II elongation factor that is conserved from yeast to humans

NDF was purified and identified as a protein that destabilizes nucleosomes (Fei et al. 2018). Consistent with this function, NDF was found to be able to facilitate Pol II transcription through a nucleosome. Here we find, unexpectedly, that NDF is a Pol II transcription factor that stimulates transcript elongation with plain DNA templates in a nucleosome-independent manner. Moreover, yeast Pdp3, which is related to NDF, binds directly to Pol II, stimulates transcription elongation, and is localized to gene bodies. Thus, NDF is an ancient protein that is conserved from yeast to humans.

In humans, hNDF, which is encoded by the *GLYR1* gene, is present at high levels in all (45/45) tested tissues (The Human Protein Atlas; Uhlen et al. 2017). This property suggests that hNDF has a widespread biological function. Upon transcriptional induction, NDF is recruited to the transcribed regions of thousands of genes, but not all induced genes, in mammalian cells (Fei et al. 2018). Its conserved PWWP motif, which binds to methylated lysines (Qin and Min 2014), is probably important for the association of NDF with its target genes, but it should also be noted that NDF is not enriched at many genes that have moderate to high levels of H3K36me3 (Fei et al. 2018). It thus seems likely that other factors, such as those associated with the transcription process, additionally contribute to the recruitment of NDF to genes during transcription. In this regard, the direct interaction between NDF and Pol II may contribute to the recruitment of NDF to gene bodies.

There are many different transcription factors that bind directly to Pol II and facilitate the elongation process (for reviews, see, for example: Sims et al. 2004; Guo and Price 2013; Chen et al. 2018; Cramer 2019; Conaway and Conaway 2019; Roeder 2019; Lis 2019; Schier and Taatjes 2020). These Pol II-binding elongation factors can be placed into two general categories. The first group comprises TFIIS and CSB, which rescue arrested and backtracked Pol II, and second group includes TFIIF, ELL, Elongin, and Spt4-Spt5, which suppress transient Pol II pausing. ELL, Elongin, and Spt4-Spt5 are also localized over gene bodies. Given that NDF functions differently than TFIIS and is localized over gene bodies, it appears that NDF and Pdp3 may act similarly to ELL, Elongin, and Spt4-Spt5. With this working hypothesis, it will be important to carry out structural, biochemical, and genetic experiments on NDF and Pdp3 that will shed additional light on their mechanisms and biological functions.

Materials and methods

Antibodies

Rabbit polyclonal antisera against hNDF were described in Fei et al. (2018). Commercial antibodies were as follows: anti-BrdU (BD Biosciences; 555627; 5 µL per sample for nascent RNA sequencing) and anti-Pol II (Santa Cruz Biotechnology; sc-9001; rabbit polyclonal antibodies raised against amino acids 1-224 of the largest subunit of human Pol II; 1:1000 dilution for western blots). Horseradish peroxidase (HRP)-conjugated protein A was obtained from ThermoFisher (101023).

Cell culture

HeLa cells were cultured by using Dulbecco's modified Eagle's medium (DMEM) containing 10% (v/v) fetal bovine serum (FBS; Gibco), 100 units/mL penicillin, and 0.1 mg/mL streptomycin. Cells were maintained in a humidified incubator atmosphere at 37 °C with 5% CO_2. NDF knockout (KO) HeLa cells were described in Fei et al. (2018).

Nucleic acids

For transcription elongation experiments, template strand (TS), non-template strand (NTS), RNA primer, and 5S rDNA sequences were used as described (Fei et al. 2018; Xu et al. 2017). The Friedreich's ataxia (*FXN*) gene fragment containing about 400 GAA trinucleotide repeats was amplified (forward primer: 5'-ATACCGGATCCGGGATTGGTTGCCAGTGCTTAAAAGTTAG-3', BamHI site is underlined; reverse primer: 5'-GGTATGGTACCGATCTAAGGACCATCATGGCCACACTTGCC-3', KpnI site is underlined) from DNA obtained from GM16223 Friedreich's ataxia patient cells (Coriell Institute for Medical Research) by using the PCR conditions described in Campuzano et al. (1996) and subcloned into the BamHI and KpnI sites of pBS (BlueScribe, Stratagene) to give

the pFXN-GAA plasmid. The pause rescue experiments with the site-specific 9A pause site were performed as previously described (Xu et al. 2017). The oligonucleotides were as follows: primer RNA (5'-AUCGAGAGGA-3'); template strand DNA (5'-CAGACTCTAACCACACATCACTTACCCTACATACACCACACACCACACCGAGAAAAAAAAAT TACCCCTTCACCCTCACTGCCCCACATCATCACTTACCTGGATACACCCTTACTCCTCTCGA TACCTCACCACCTTACCTACCACCCAC-3'); biotin-labeled non-template strand DNA (5'-biotin-TTTGTGGGTGGTAGGTAAGGTGGTGAGGTATCGAGAGGAGTAAGGGTGTATCCAGGTAAG TGATGATGTGGGGCAGTGAGGGTGAAGGGGTAATTTTTTTTTCTCGGTGTGGTGTGTGGT GTATGTAGGGTAAGTGATGTGTGGTTAGAGTCTG-3').

Additional methods are included in the Supplemental Material. The genome-wide data have been deposited at the Gene Expression Omnibus (GEO; accession number GSE185464), and will be released upon acceptance of the paper for publication. All experiments were performed independently at least two times to ensure reproducibility of the data.

Acknowledgments

We thank E. Peter Geiduschek, Long Vo ngoc, Grisel Cruz-Becerra, and Torrey Rhyne for critical reading of the manuscript. J.T.K. is the Amylin Chair in the Life Sciences. This work was supported by NIH grant R35 GM118060 to J.T.K. and NIH grant R01 GM102362 to D.W.

References

Ardehali MB, Damle M, Perea-Resa C, Blower MD, Kingston RE. 2021. Elongin A associates with actively transcribed genes and modulates enhancer RNA levels with limited impact on transcription elongation rate in vivo. *J Biol Chem* **296:** 100202.

Bidichandani SI, Ashizawa T, Patel PI. 1998. The GAA triplet-repeat expansion in Friedreich ataxia interferes with transcription and may be associated with an unusual DNA structure. *Am J Hum Genet* **62:** 111-121.

Campuzano V, Montermini L, Molto MD, Pianese L, Cossee M, Cavalcanti F, Monros E, Rodius F, Duclos F, Monticelli A, et al. 1996. Friedreich's ataxia: autosomal recessive disease caused by an intronic GAA triplet repeat expansion. *Science* **271:** 1423-1427.

Chen FX, Smith ER, Shilatifard A. 2018. Born to run: control of transcription elongation by RNA polymerase II. *Nat Rev Mol Cell Biol* **19:** 464-478.

Conaway RC, Conaway JW. 2019. The hunt for RNA polymerase II elongation factors: a historical perspective. *Nat Struct Mol Biol* **26:** 771-776.

Cramer P. 2019. Organization and regulation of gene transcription. *Nature* **573:** 45-54.

Fang R, Chen F, Dong Z, Hu D, Barbera AJ, Clark EA, Fang J, Yang Y, Mei P, Rutenberg M, et al. 2013. LSD2/KDM1B and its cofactor NPAC/GLYR1 endow a structural and molecular model for regulation of H3K4 demethylation. *Mol Cell* **49:** 558-570.

Fei J, Ishii H, Hoeksema MA, Meitinger F, Kassavetis GA, Glass CK, Ren B, Kadonaga JT. 2018. NDF, a nucleosome-destabilizing factor that facilitates transcription through nucleosomes. *Genes Dev* **32:** 682-694.

Flury V, Georgescu PR, Iesmantavicius V, Shimada Y, Kuzdere T, Braun S, Bühler M. 2017. The histone acetyltransferase Mst2 protects active chromatin from epigenetic silencing by acetylating the ubiquitin ligase Brl1. *Mol Cell* **67:** 294-307.

Gilbert TM, McDaniel SL, Byrum SD, Cades JA, Dancy BC, Wade H, Tackett AJ, Strahl BD, Taverna SD. 2014. A PWWP domain-containing protein targets the NuA3

acetyltransferase complex via histone H3 lysine 36 trimethylation to coordinate transcriptional elongation at coding regions. *Mol Cell Proteomics* **13:** 2883-2895.

Gopalan S, Gibbon DM, Banks CA, Zhang Y, Florens LA, Washburn MP, Dabas P, Sharma N, Seidel CW, Conaway RC, et al. 2018. *Schizosaccharomyces pombe* Pol II transcription elongation factor ELL functions as part of a rudimentary super elongation complex. *Nucleic Acids Res* **46:** 10095-10105.

Guo J, Price DH. 2013. RNA polymerase II elongation control. *Chem Rev* **113:** 8583-8603.

Kireeva ML, Komissarova N, Waugh DS, Kashlev M. 2000. The 8-nucleotide-long RNA:DNA hybrid is a primary stability determinant of the RNA polymerase II elongation complex. *J Biol Chem* **275:** 6530-6536.

Komissarova N, Kireeva ML, Becker J, Sidorenkov I, Kashlev M. 2003. Engineering of elongation complexes of bacterial and yeast RNA polymerases. *Methods Enzymol* **371:** 233-251.

Li Y, Lu Y, Polak U, Lin K, Shen J, Farmer J, Seyer L, Bhalla AD, Rozwadowska N, Lynch DR, et al. 2015. Expanded GAA repeats impede transcription elongation through the *FXN* gene and induce transcriptional silencing that is restricted to the *FXN* locus. *Hum Mol Genet* **24:** 6932-6943.

Lis JT. 2019. A 50 year history of technologies that drove discovery in eukaryotic transcription regulation. *Nat Struct Mol Biol* **26:** 777-782.

Nudler E. 2012. RNA polymerase backtracking in gene regulation and genome instability. *Cell* **149:** 1438-1445.

Paulsen MT, Veloso A, Prasad J, Bedi K, Ljungman EA, Tsan YC, Chang CW, Tarrier B, Washburn JG, Lyons R, et al. 2013. Coordinated regulation of synthesis and stability of RNA during the acute TNF-induced proinflammatory response. *Proc Natl Acad Sci* **110:** 2240-2245.

Punga T, Buhler M. 2010. Long intronic GAA repeats causing Friedreich ataxia impede transcription elongation. *EMBO Mol Med* **2:** 120-129.

Qin S, Min J. 2014. Structure and function of the nucleosome-binding PWWP domain. *Trends Biochem Sci* **39**: 536-547.

Reinberg D, Roeder RG. 1987. Factors involved in specific transcription by mammalian RNA polymerase II. Transcription factor IIS stimulates elongation of RNA chains. *J Biol Chem* **262:** 3331-3337.

Roeder RG. 2019. 50+ years of eukaryotic transcription: an expanding universe of factors and mechanisms. *Nat Struct Mol Biol* **26:** 783-791.

Schier AC, Taatjes DJ. 2020. Structure and mechanism of the RNA polymerase II transcription machinery. *Genes Dev* **34:** 465-488.

Sekimizu K, Kobayashi N, Mizuno D, Natori S. 1976. Purification of a factor from Ehrlich ascites tumor cells specifically stimulating RNA polymerase II. *Biochemistry* **15:** 5064-5070.

Sheridan RM, Fong N, D'Alessandro A, Bentley DL. 2019. Widespread backtracking by RNA Pol II is a major effector of gene activation, 5' pause release, termination, and transcription elongation rate. *Mol Cell* **73:** 107-118.

Sidorenkov I, Komissarova N, Kashlev M. 1998. Crucial role of the RNA:DNA hybrid in the processivity of transcription. *Mol Cell* **2:** 55-64.

Sigurdsson S, Dirac-Svejstrup AB, Svejstrup JQ. 2010. Evidence that transcript cleavage is essential for RNA polymerase II transcription and cell viability. *Mol Cell* **38:** 202-210.

Sims RJ 3rd, Belotserkovskaya R, Reinberg D. 2004. Elongation by RNA polymerase II: the short and long of it. *Genes Dev* **18:** 2437-2468.

Uhlen M, Zhang C, Lee S, Sjöstedt E, Fagerberg L, Bidkhori G, Benfeitas R, Arif M, Liu Z, Edfors F, et al. 2017. A pathology atlas of the human cancer transcriptome. *Science* **357:** eaan2507.

Vermeulen M, Eberl HC, Matarese F, Marks H, Denissov S, Butter F, Lee KK, Olsen JV, Hyman AA, Stunnenberg HG, et al. 2010. Quantitative interaction proteomics and genome-wide profiling of epigenetic histone marks and their readers. *Cell* **142:** 967-980.

Wang CI, Alekseyenko AA, LeRoy G, Elia AE, Gorchakov AA, Britton LM, Elledge SJ, Kharchenko PV, Garcia BA, Kuroda MI. 2013. Chromatin proteins captured by ChIP-mass spectrometry are linked to dosage compensation in *Drosophila*. *Nat Struct Mol Biol* **20:** 202-209.

Wang Y, Hou L, Ardehali MB, Kingston RE, Dynlacht BD. 2021. Elongin A regulates transcription in vivo through enhanced RNA polymerase processivity. *J Biol Chem* **296:** 100170.

Wind M, Reines D. 2000. Transcription elongation factor SII. *Bioessays* **22:** 327-336.

Xu J, Lahiri I, Wang W, Wier A, Cianfrocco MA, Chong J, Hare AA, Dervan PB, DiMaio F, Leschziner AE, et al. 2017. Structural basis for the initiation of eukaryotic transcription-coupled DNA repair. *Nature* **551:** 653-657.

Figure Legends

Figure 1. NDF stimulates non-specific in vitro transcription by purified yeast Pol II (yPol II) and binds to human Pol II (hPol II) in cell extracts. (*A, B*) Stimulation of in vitro Pol II transcription by hNDF and dNDF, respectively. (*C, D*) Time course of transcription in the presence (red dots) or absence (blue dots) of hNDF and dNDF, respectively. For *A*-*D*, reactions were carried out as depicted in Supplemental Fig. S1A, and the primary data are given in Supplemental Table S1. Three replicate reactions were performed for each condition. Each cluster of dots corresponds to a single reaction condition (in *A,* the 6.25 nM hNDF data points are colored green to distinguish them from the red 12.5 nM hNDF data points). The standard deviation (error bars) and mean (central horizontal line) are indicated. The lines connect the mean values. (*E)* FLAG-hNDF-GFP co-immunoprecipitates with endogenous hPol II In HeLa cells. Lysates from cells containing FLAG-hNDF-GFP were incubated with FLAG M2 antibodies or IgG control. The immunoprecipitated proteins were subjected to western blot analysis with anti-FLAG and anti-Rpb1 (Pol II) antibodies. (*F*) Co-immunoprecipitation of endogenous hNDF and hPol II. HeLa whole cell lysates were incubated with anti-hNDF polyclonal antibodies (or pre-immune serum as the control) and Dynabeads Protein A. The beads were washed, and the associated proteins were subjected to western blot analysis.

Figure 2. hNDF stimulates transcription elongation by purified human Pol II. (*A*) Diagram of the assay with purified Pol II elongation complexes. The transcripts were analyzed by denaturing 8% polyacrylamide–urea gel electrophoresis. (*B*) Transcription elongation reactions with purified HeLa Pol II and the *Xenopus borealis* 5S rDNA template. Reactions were performed in the presence or absence of purified hNDF for the indicated times. (*C*) Transcription elongation reactions with purified HeLa Pol II and a patient-derived human *FXN* gene segment containing about 400 GAA trinucleotide repeats. The estimated location of the GAA repeats is shown. The concentrations of purified hNDF protein and reaction times are indicated.

Figure 3. NDF-mediated Pol II stimulation is distinct from TFIIS-mediated rescue of backtracked Pol II. (*A*) Diagram of the Pol II elongation system used in these experiments. The downstream 9A sequence is in the template strand and induces Pol II pausing and backtracking. The 9A-paused transcripts and the full-length run-off transcripts were resolved by denaturing 8% polyacrylamide–urea gel electrophoresis. (*B*) NDF has little effect upon the transcription of Pol II through the 9A pause site. (*C*) TFIIS, but not NDF, can rescue purified arrested Pol II elongation complexes. The arrested Pol II complexes were treated with hNDF or yTFIIS in the presence of rNTPs for the indicated times. Cleaved and extended transcripts can be seen with TFIIS but not with NDF. (*D*) Unlike TFIIS, NDF cannot stimulate the RNA endonuclease activity of Pol II. Purified arrested Pol II elongation complexes were treated with hNDF or yTFIIS in the absence of rNTPs. The cleavage of the transcripts can be seen with TFIIS but not with NDF.

Figure 4. NDF has a small but distinct effect upon ongoing Pol II transcription in cells. Transcription in wild-type (WT) versus NDF knockout (KO) HeLa cells was assessed by incubation of the cells for 10 min with 5-bromouridine (Bru-seq analysis; Paulsen et al. 2013). The gene clusters were generated by k-means clustering of NDF ChIP-seq, H3K36me3 ChIP-seq, and RNA-seq data obtained with wild-type HeLa cells (Fei et al. 2018). Cluster 1 contains active genes that have high levels of NDF and H3K36me3. Cluster 2 has active genes with medium to low levels of NDF and H3K36me3. Clusters 3 and 4 contain genes with low or very low levels of activity, respectively. (*A*) NDF has a small but distinct effect upon transcription in genes that contain high levels of NDF in WT cells. The log2 of the Bru-seq signal in KO cells versus WT cells is plotted against log10 of the NDF ChIP-seq signal in WT cells. (*B*) Comparison of the Bru-seq signal in KO versus WT cells to the RNA-seq signal in WT cells.

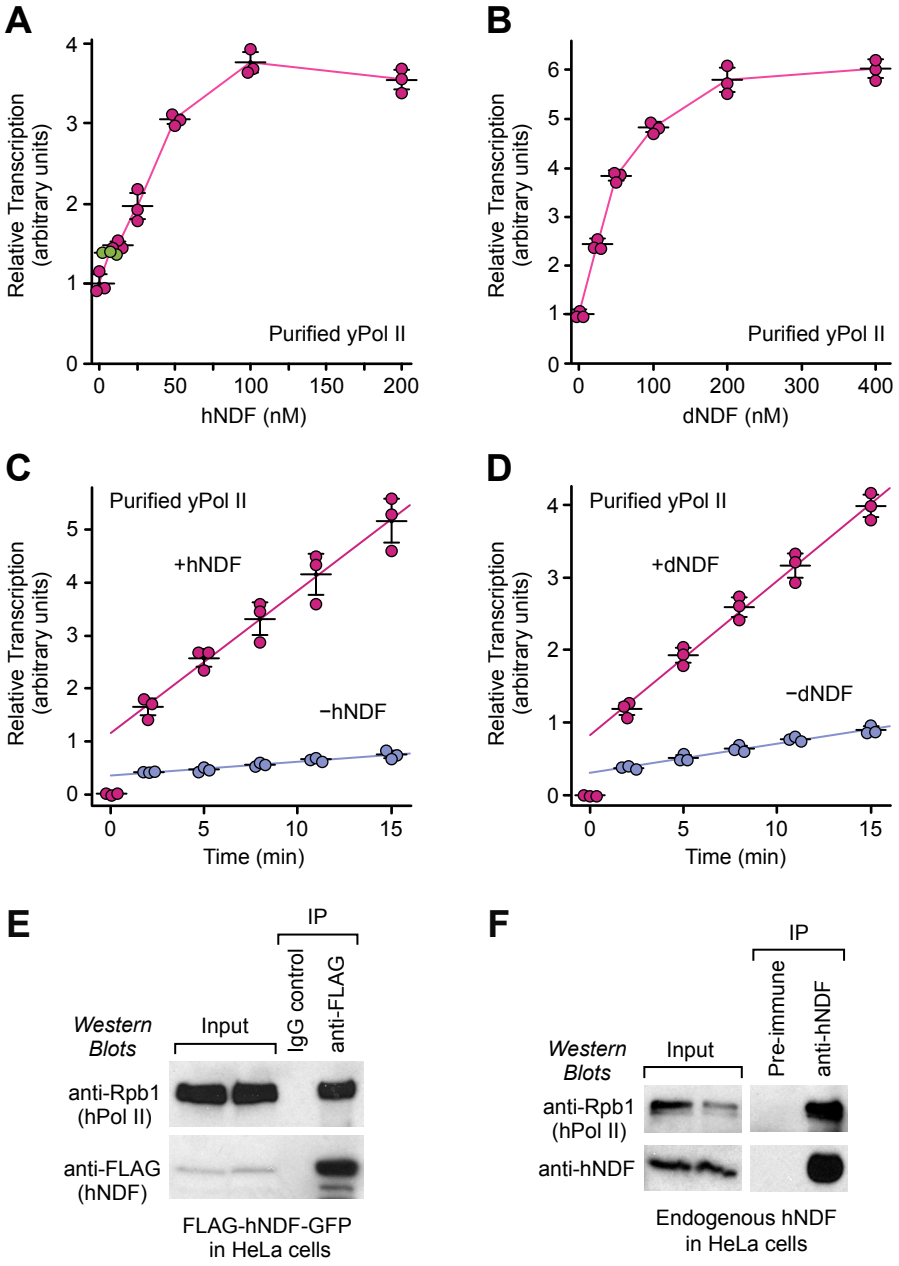
A
Relative Transcription (arbitrary units)
Purified yPol II
hNDF (nM)
B
Relative Transcription (arbitrary units)
Purified yPol II
dNDF (nM)
C
Purified yPol II
+hNDF
−hNDF
Relative Transcription (arbitrary units)
Time (min)
D
Purified yPol II
+dNDF
−dNDF
Relative Transcription (arbitrary units)
Time (min)
E
IP
IgG control
anti-FLAG
Western Blots
Input
anti-Rpb1 (hPol II)
anti-FLAG (hNDF)
FLAG-hNDF-GFP in HeLa cells
F
IP
Pre-immune
anti-hNDF
Western Blots
Input
anti-Rpb1 (hPol II)
anti-hNDF
Endogenous hNDF in HeLa cells

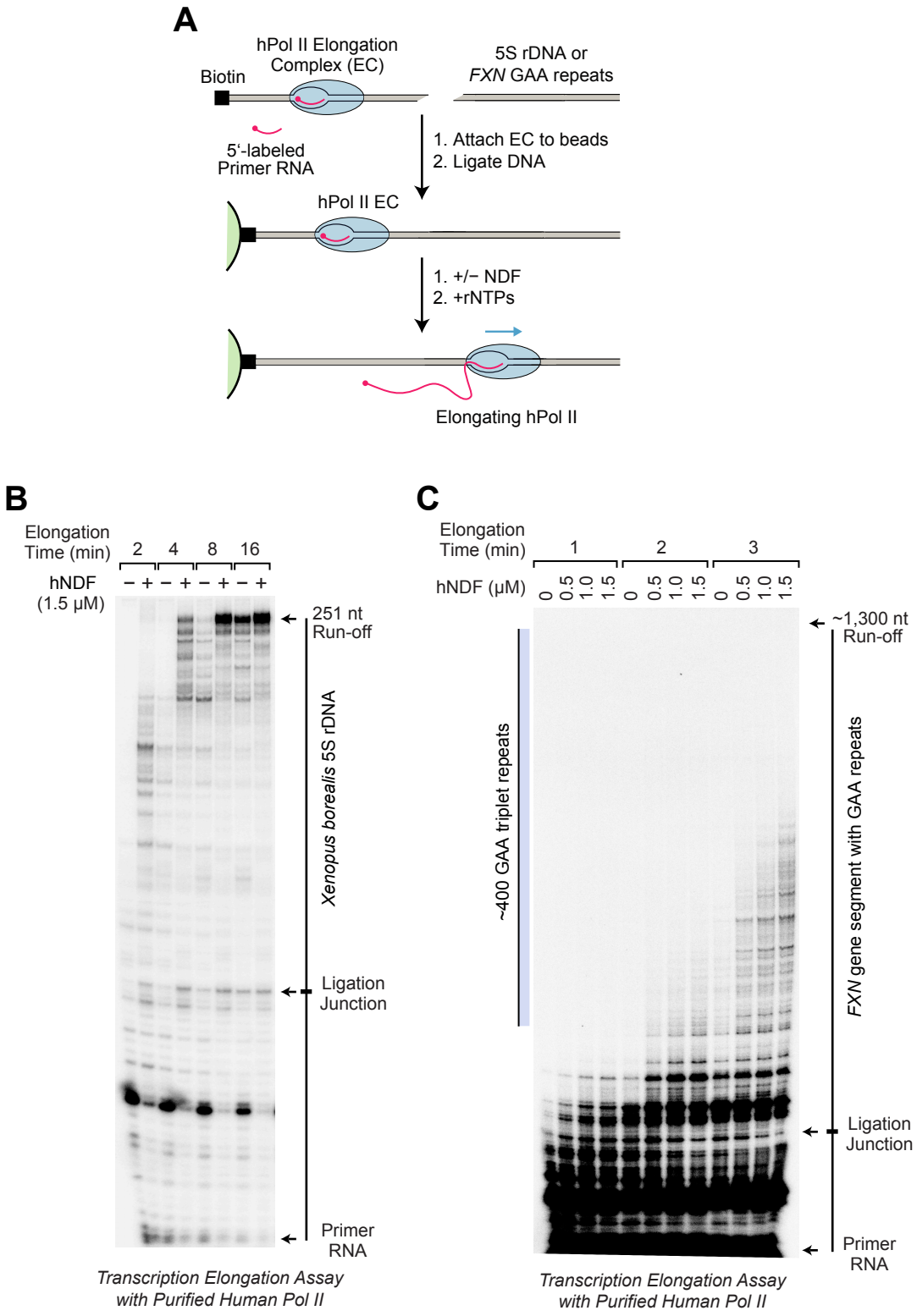
A
hPol II Elongation Complex (EC)
Biotin
5S rDNA or FXN GAA repeats
5'-labeled Primer RNA
1. Attach EC to beads
2. Ligate DNA
hPol II EC
1. +/− NDF
2. +rNTPs
Elongating hPol II
B
Elongation Time (min)
2 4 8 16
hNDF (1.5 μM)
− + − + − + − +
251 nt Run-off
Xenopus borealis 5S rDNA
Ligation Junction
Primer RNA
Transcription Elongation Assay with Purified Human Pol II
C
Elongation Time (min)
1 2 3
hNDF (μM)
0 0.5 1.0 1.5 0 0.5 1.0 1.5 0 0.5 1.0 1.5
~400 GAA triplet repeats
~1,300 nt Run-off
FXN gene segment with GAA repeats
Ligation Junction
Primer RNA
Transcription Elongation Assay with Purified Human Pol II

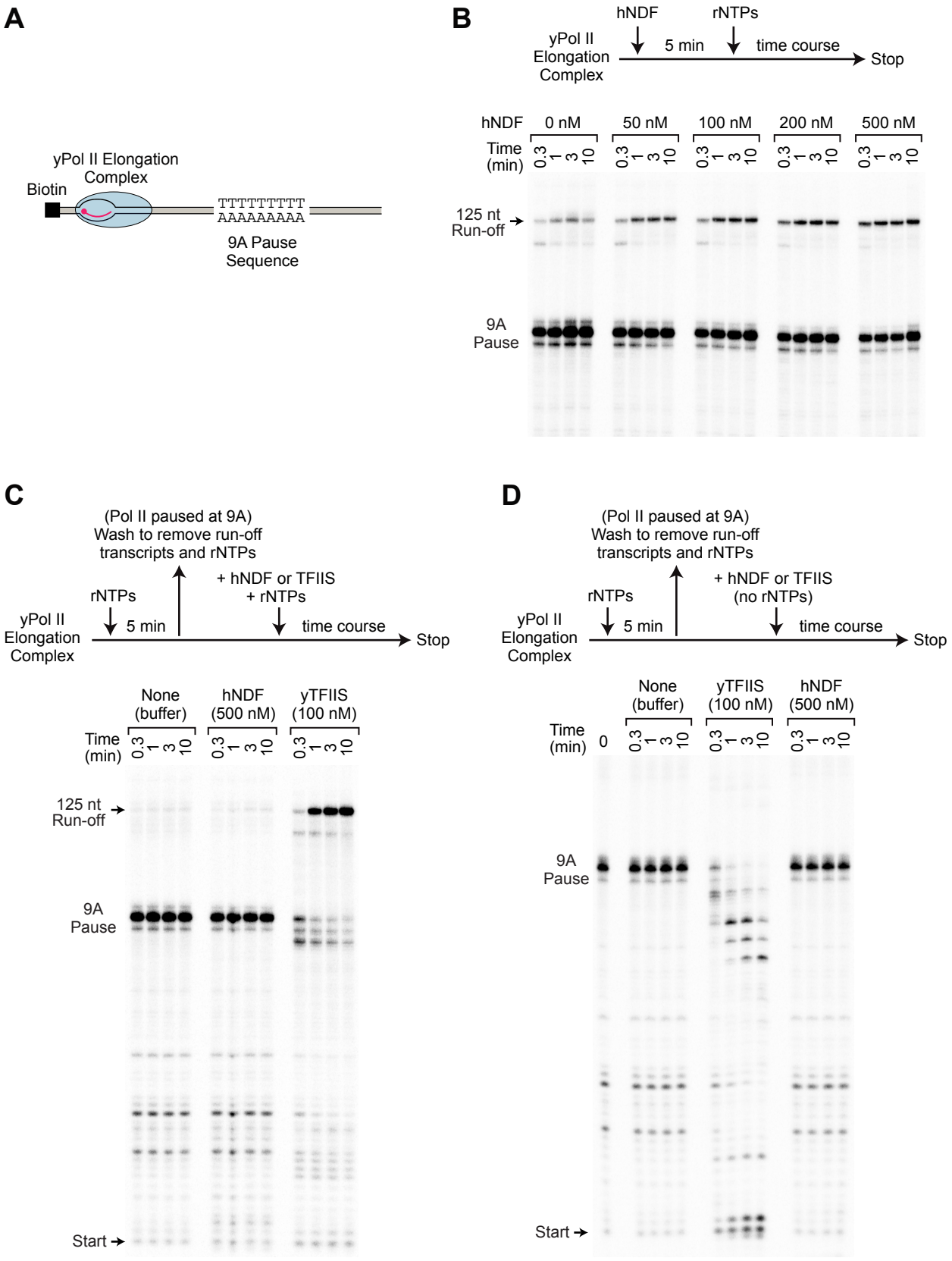
A
yPol II Elongation Complex
Biotin
TTTTTTTTT
AAAAAAAAA
9A Pause Sequence
B
hNDF
rNTPs
yPol II Elongation Complex
5 min
time course
Stop
hNDF
0 nM
50 nM
100 nM
200 nM
500 nM
Time (min)
0.3
1
3
10
125 nt Run-off
9A Pause
C
(Pol II paused at 9A)
Wash to remove run-off transcripts and rNTPs
rNTPs
+ hNDF or TFIIS + rNTPs
yPol II Elongation Complex
5 min
time course
Stop
None (buffer)
hNDF (500 nM)
yTFIIS (100 nM)
Time (min)
125 nt Run-off
9A Pause
Start
D
(Pol II paused at 9A)
Wash to remove run-off transcripts and rNTPs
rNTPs
+ hNDF or TFIIS (no rNTPs)
yPol II Elongation Complex
5 min
time course
Stop
None (buffer)
yTFIIS (100 nM)
hNDF (500 nM)
Time (min)
0
9A Pause
Start

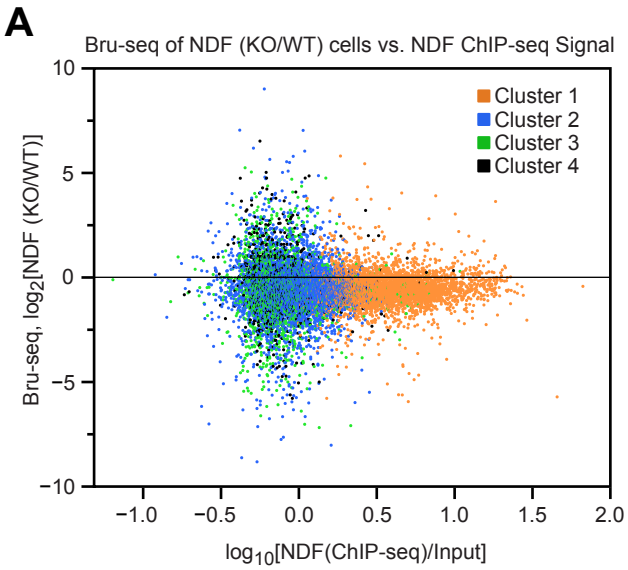
A
Bru-seq of NDF (KO/WT) cells vs. NDF ChIP-seq Signal
Cluster 1
Cluster 2
Cluster 3
Cluster 4
Bru-seq, log2[NDF (KO/WT)]
log10[NDF(ChIP-seq)/Input]
10
5
0
−5
−10
−1.0
−0.5
0.0
0.5
1.0
1.5
2.0

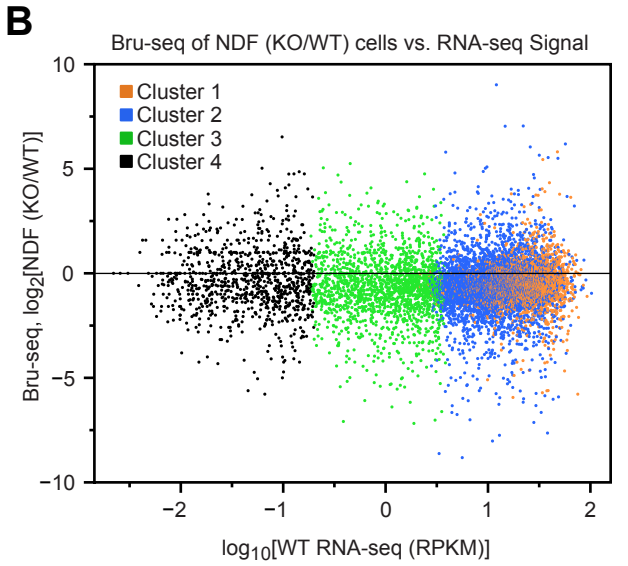
B
Bru-seq of NDF (KO/WT) cells vs. RNA-seq Signal
Cluster 1
Cluster 2
Cluster 3
Cluster 4
Bru-seq, log2[NDF (KO/WT)]
log10[WT RNA-seq (RPKM)]
10
5
0
−5
−10
−2
−1
0
1
2

SUPPLEMENTAL MATERIAL

NDF Is a Transcription Factor that Stimulates Elongation by RNA Polymerase II

Jia Fei, Jun Xu, Ziwei Li, Kevin Xu, Dong Wang, George A. Kassavetis,
and James T. Kadonaga

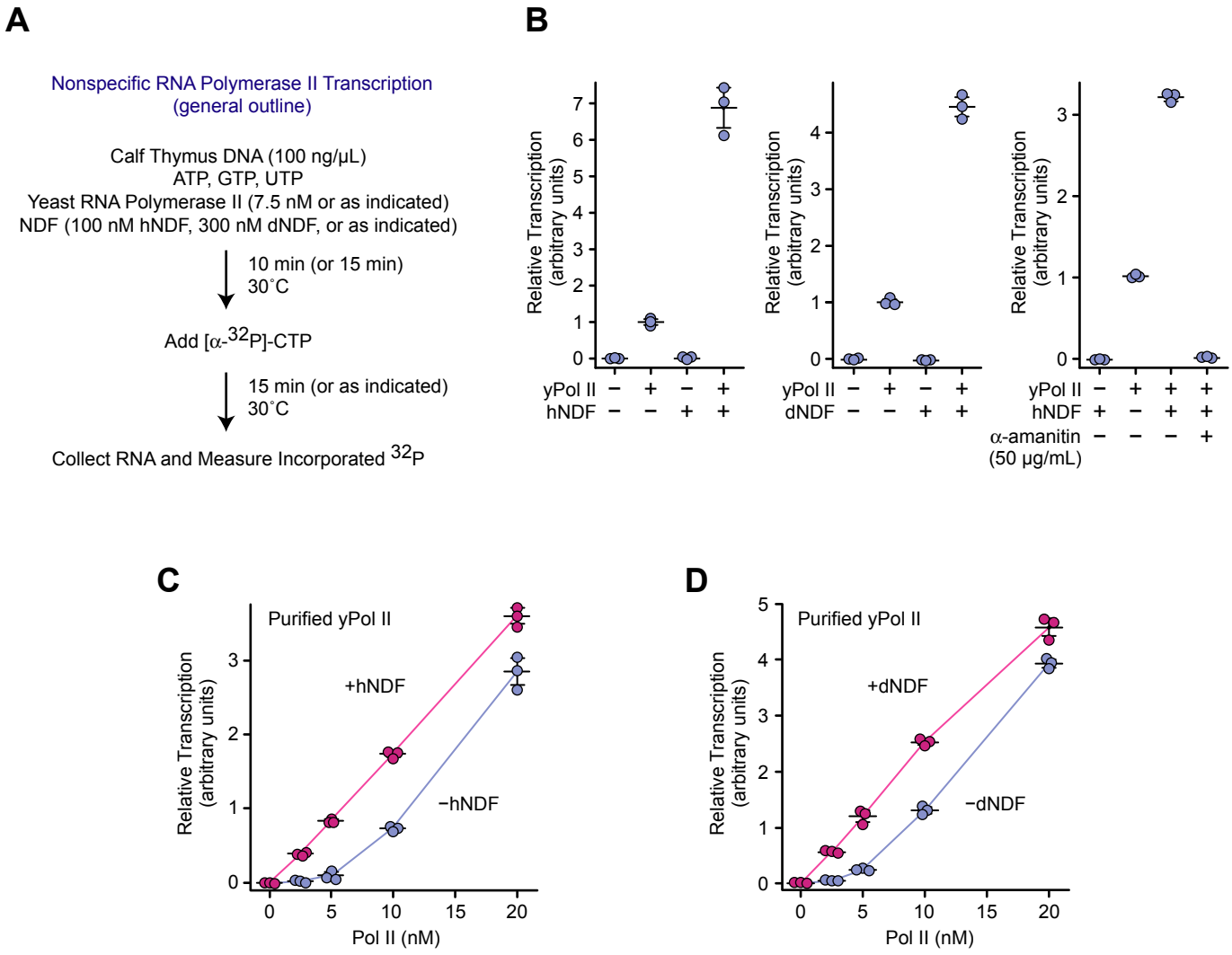

Supplemental Figure S1. Analysis of NDF-mediated stimulation of non-specific transcription by purified yeast Pol II (yPol II). (*A*) Schematic diagram of the non-specific transcription assay. The standard conditions are shown. In any series of reactions, identical conditions were used except for the indicated variables. (*B*) NDF and Pol II preparations lack contaminating polymerases. Purified hNDF alone (left panel) and dNDF alone (middle panel) do not exhibit transcription activity. Transcription by yeast Pol II is inhibited by 50 μM α-amanitin (right panel), which indicates the absence of Pol I and Pol III. (*C*, *D*) Analysis of transcription at different Pol II concentrations in the presence (red dots) or absence (blue dots) of hNDF and dNDF, respectively. In our standard reactions, we used a Pol II concentration of 7.5 nM, which is in the linear concentration-activity range. The primary data are given in Supplemental Table S1.

Supplemental Figure S2. Sequence alignment of *Saccharomyces cerevisiae* Pdp3 (yPdp3) and human NDF (hNDF). The full-length sequence of yPdp3 from *S. cerevisiae* strain S288C was aligned with the full-length sequence of hNDF by using EMBOSS Needle (https://www.ebi.ac.uk/Tools/psa/emboss_needle/). This alignment reveals that yPdp3 has extensive sequence similarity (25% identity, 76/304; 39% similarity, 119/304) with the N-terminal region of hNDF and lacks the catalytically-inactive dehydrogenase domain at the C-terminus of hNDF (highlighted in BLUE type). The PWWP domain in hNDF is denoted by RED type. The functional PWWP domain in yPdp3, as defined by Gilbert et al. (2014), is shown in GREEN type.

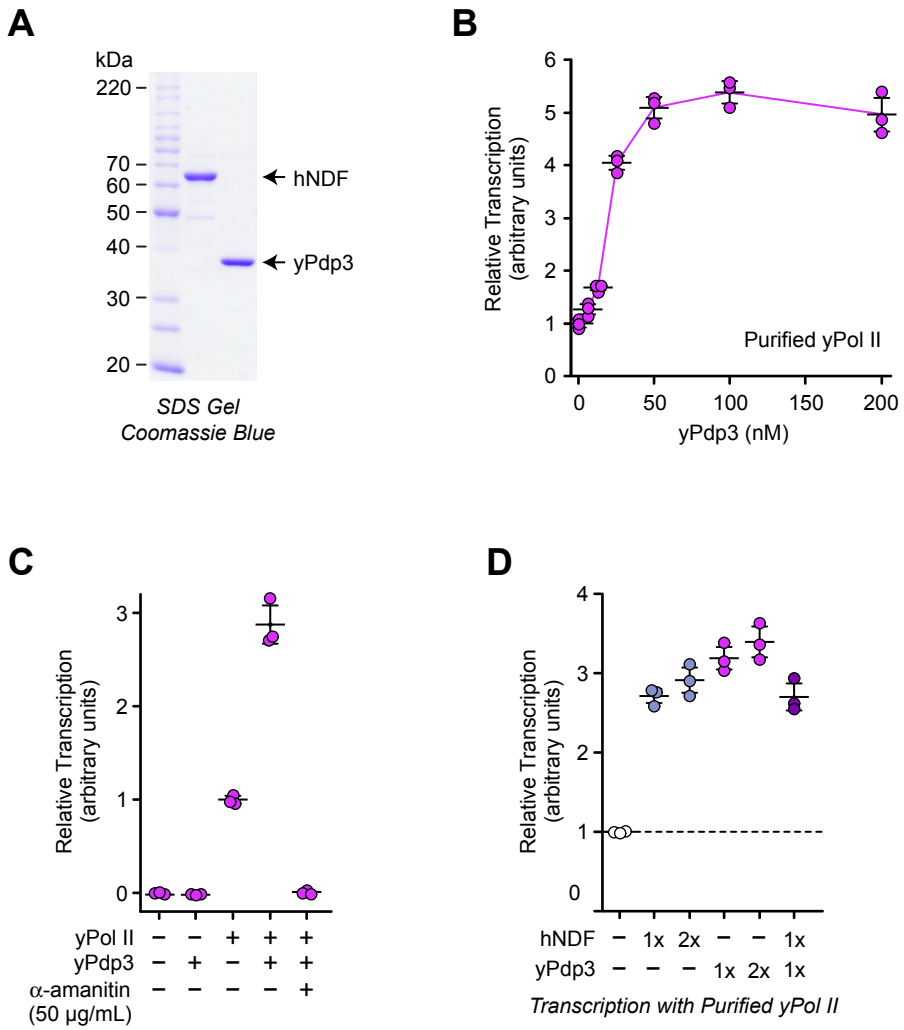

Supplemental Figure S3. Purified *S. cerevisiae* Pdp3 protein (yPdp3) stimulates transcription by purified *S. cerevisiae* RNA polymerase II (yPol II). (*A*) Purification of full-length yPdp3 protein. His6-yPdp3-FLAG protein (yPdp3) was purified by the same method that was developed for the purification of His6-hNDF-FLAG (hNDF), as described in the Supplemental Materials and Methods. This figure shows 10% polyacrylamide-SDS gel analysis of both protein preparations. (*B*) Stimulation of in vitro Pol II transcription by yPdp3. Standard transcription reactions were performed with the indicated concentrations of yPdp3, as in Figs. 1A and 1B and outlined in Supplemental Fig. S1A. (*C*) Control transcription reactions show that yPdp3 alone lacks transcription activity and that transcription with purified yPdp3 and Pol II is being carried out by RNA polymerase II. Standard conditions were employed, as in Supplemental Figs. S1A and S1B. (*D*) hNDF and yPdp3 do not exhibit transcriptional synergy. 1x hNDF and 1x yPdp3 each correspond to 50 nM. We have also performed reactions with 4x hNDF, 4x yPdp3, and 2x hNDF + 2x yPdp3. The additional reactions lead to the same conclusions as the data shown in *D*. For the in vitro transcription experiments in this figure, three replicate reactions were performed for each condition. Each cluster of dots corresponds to a single reaction condition. The standard deviation (error bars) and mean (central horizontal line) are indicated. In panel *B*, the lines connect the mean values. The primary data are given in Supplemental Table S1.

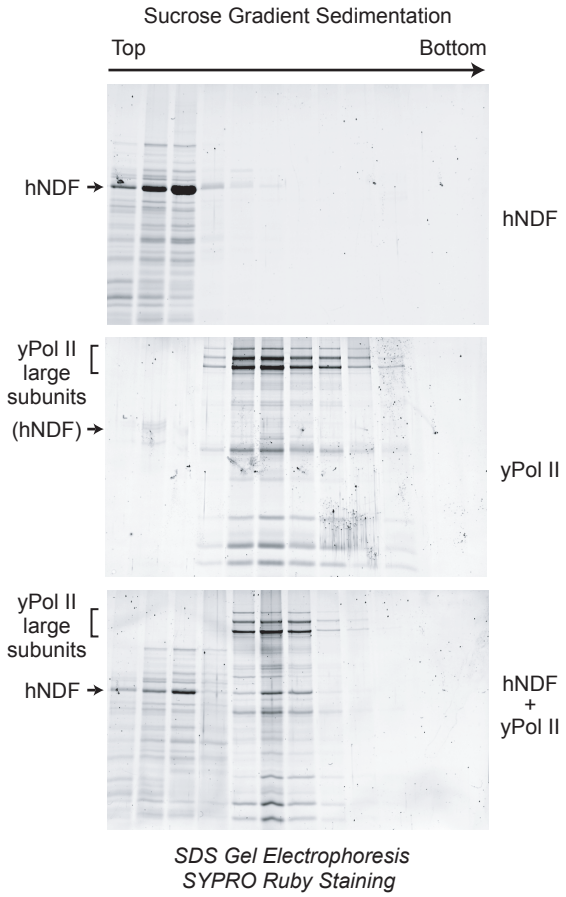

Supplemental Figure S4. Purified hNDF binds directly to purified yeast Pol II. Sucrose gradient sedimentation experiments were performed with hNDF (150 pmol; top panel), yPol II (10 pmol; middle panel), and both hNDF (150 pmol) and yPol II (10 pmol) (bottom panel). The samples were subjected to 10 to 30% (w/v, left to right) sucrose gradient sedimentation in a Beckman SW41 rotor (32,000 rpm, 4 °C, 18 h). The proteins were analyzed by SDS-polyacrylamide gel electrophoresis and staining with SYPRO Ruby.

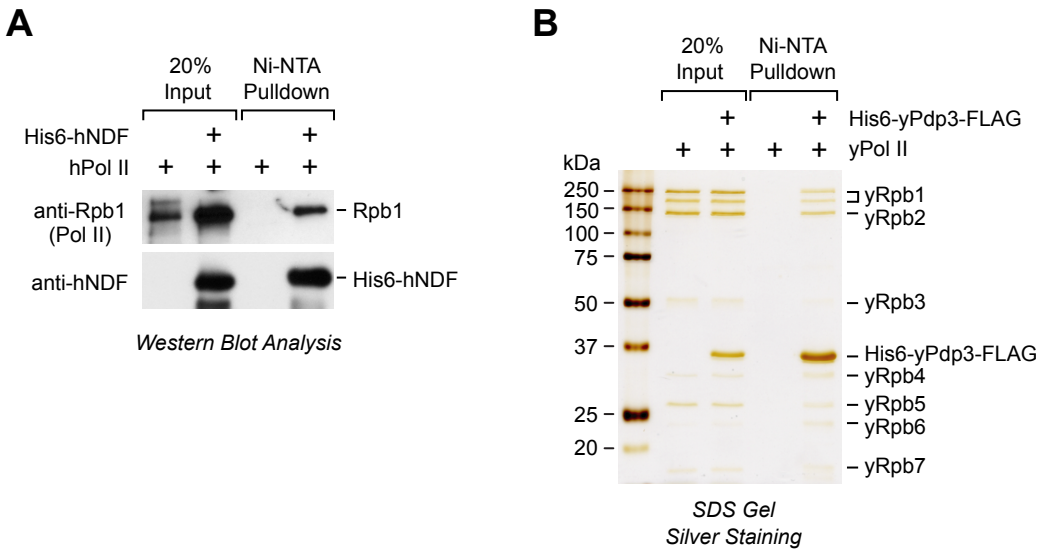

Supplemental Figure S5. Human NDF (hNDF) and *S. cerevisiae* Pdp3 (yPdp3) bind directly to RNA polymerase II. (*A*) Purified hNDF interacts with purified human RNA polymerase II (hPol II). Purified hPol II in the presence or absence of purified His6-hNDF was incubated with Ni-NTA agarose beads, which were then pelleted. The bound proteins were subjected to western blot analysis with the indicated antibodies. (*B*) Purified yPdp3 interacts with purified yeast RNA polymerase II (yPol II). Purified yPol II in the presence or absence of purified His6-yPdp3-FLAG protein was incubated with Ni-NTA agarose beads, which were then pelleted. The bound proteins were subjected to 10% polyacrylamide-SDS gel electrophoresis and visualized by silver staining. The bands that correspond to His6-yPdp3-FLAG and the Rpb1 to Rpb7 subunits of yPol II are indicated.

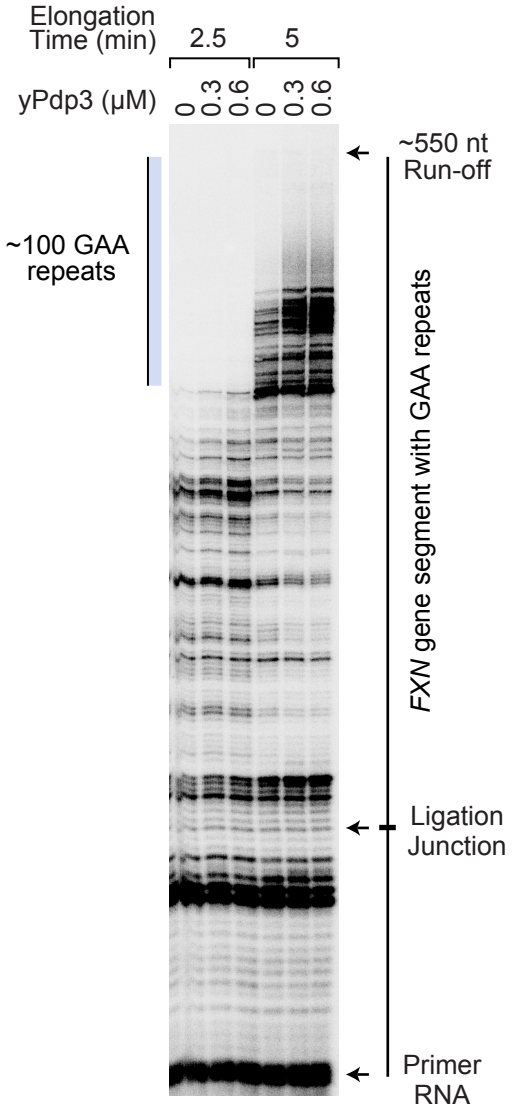

Transcription Elongation Assay with Purified Human Pol II

Supplemental Figure S6. yPdp3 stimulates transcription elongation by purified human Pol II. Transcription elongation assays were performed with purified yPdp3 and purified hPol II as in Figs. 2A and 2C of the main text but with a downstream *FXN* sequence that contains ~100 copies of the GAA triplet repeats. The estimated location of the GAA repeats is indicated.

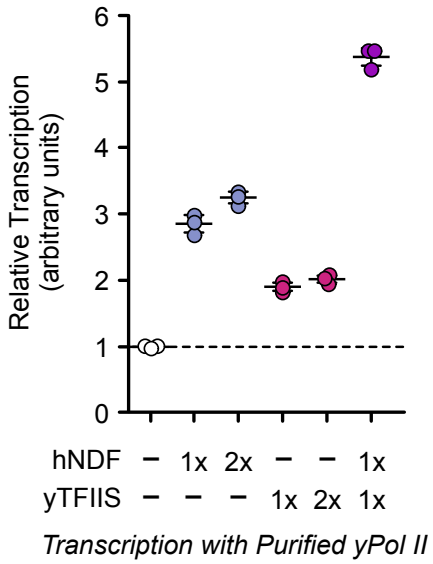

Supplemental Figure S7. The combination of NDF and TFIIS yields higher levels of transcription than either factor alone. Transcription reactions were performed under standard conditions with purified yeast RNA polymerase II (7.5 nM; yPol II) and calf thymus DNA (100 ng/μL), as outlined in Supplemental Fig. S1A. Where indicated, human NDF and yeast TFIIS (131-309), which has complete transcriptional activity of full-length yTFIIS (Olmsted et al. 1998), were included in the reactions. 1x hNDF corresponds to 50 nM, and 1x TFIIS corresponds to 25 nM. Three replicate reactions were performed for each condition. Each cluster of dots corresponds to a single reaction condition. The standard deviation (error bars) and mean (central horizontal line) are indicated. We have also performed TFIIS alone control reactions as well as reactions with 4x hNDF, 4x TFIIS, and 2x hNDF + 2x TFIIS. The additional reactions lead to the same conclusions as the data shown above. The primary data for all of the reactions are given in Supplemental Table S1.

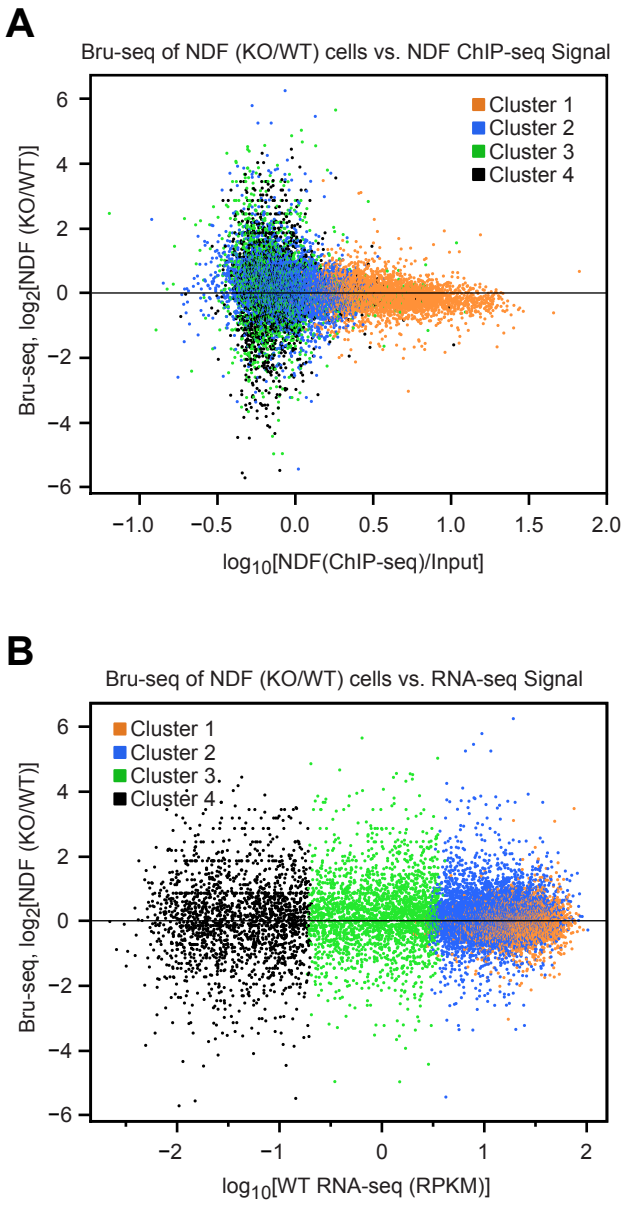

Supplemental Figure S8. NDF facilitates ongoing transcription in HeLa cells. These experiments are biological replicates of the experiments shown in Fig. 4 of the main text.

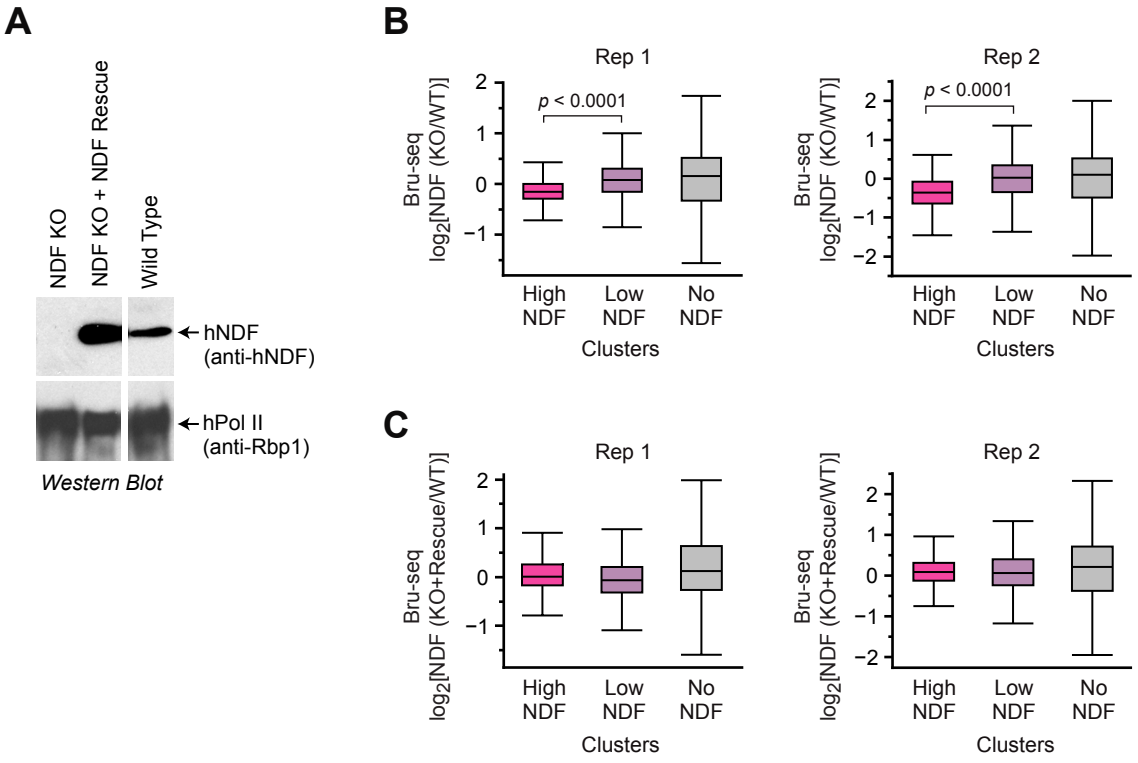

Supplemental Figure S9. The addition of NDF (NDF rescue) to NDF knockout (KO) cells results in the restoration of the loss of transcriptional activity in genes associated with high levels of NDF in human SW480 cells. (*A*) Generation of NDF knockout (KO) SW480 cells and KO+NDF rescue SW480 cells. The methodology is described in the Supplemental Materials and Methods. The expression of human NDF (hNDF) and the Rpb1 subunit of Pol II (as a control) was detected by western blot analysis. (*B*) NDF has a small effect upon ongoing transcription in SW480 cells. Transcription in wild-type (WT) versus NDF knockout (KO) SW480 cells was assessed by incubation of the cells for 10 min with 5-bromouridine (Bru-seq analysis; Paulsen et al. 2013). The High NDF, Low NDF, and No NDF gene clusters were generated based on NDF ChIP-seq signals quantified by HOMER. The High NDF cluster contains 793 genes; the Low NDF cluster contains 4,288 genes; and the No NDF cluster contains 12,733 genes. (C) The expression of recombinant NDF in the NDF KO cells results in the restoration of the loss of transcriptional activity that was seen in High NDF genes upon the loss of NDF in SW480 cells. Bru-seq experiments were performed as in *B*. In *B* and *C*, data from biological replicate experiments are shown. The sequencing data were normalized to a total of 10 million reads.

Supplemental Materials and Methods

Protein purification

Full-length His6-hNDF and His6-dNDF recombinant proteins were purified as described (Fei et al. 2018). Proteins were eluted and stored in Elution Buffer [10 mM Tris-HCl, pH 7.5, 0.2% (v/v) Nonidet P-40 (Pierce), 0.2 M NaCl, 10% (v/v) glycerol, 250 mM imidazole, and 5 mM 2-mercaptoethanol]. New methods for the purification of His6-hNDF-FLAG and His6-yPdp3-FLAG are described below. The *Saccharomyces cerevisiae* RNA polymerase II (Pol II) was purified as described (Kaplan et al. 2008). The HeLa cells that express FLAG-tagged Rpb9 subunit of Pol II was the generous gift of Dr. Robert Roeder (Rockefeller University), and the Pol II was purified as described (Malik and Roeder 2003). Recombinant yeast TFIIS protein (131-309), which has complete transcriptional activity in vitro and in vivo (Olmsted et al. 1998), was prepared as described in Awrey et al. (1998).

Purification of His6-hNDF-FLAG protein

We developed a new method for the purification of His6-hNDF-FLAG (used in the non-specific transcription assays; Figs. 1 and S1), as follows. The full-length hNDF expression plasmid, pET21b-His6-hNDF (Fei et al. 2018), was modified by the addition of a C-terminal FLAG epitope tag, GYDYKDDDDK, and transformed into Rosetta 2 (DE3) pLysS (MilliporeSigma). The cells were grown at 37°C in LB medium (0.5 L; with 80 µg/mL and 34 µg/mL, ampicillin and chloramphenicol, respectively) to an A600 nm of 0.8, induced with IPTG to 0.5 mM final concentration, grown for an additional 2 hours, and harvested by centrifugation (Fiberlite F14S-6x250y rotor; 10,000 rpm; 15 min; 4°C). Unless stated otherwise, the remaining operations were carried out at 4°C. The cells (~1 g wet mass) were resuspended in 7 mL Lysis Buffer [40 mM potassium phosphate, pH 7.6, 0.01% (v/v) Nonidet P-40 (Pierce), 0.1 mM EDTA, 580 mM NaCl, 10% (v/v) glycerol, 10 mM 2-mercaptoethanol, 1 µg/mL leupeptin, 1 µg/mL pepstatin, 0.5 mM PMSF, and 300 µg/mL lysozyme], incubated for 30 min on ice, sonicated (Branson Sonifier 450

with a 0.125 inch microtip; 20% output; 10 cycles of sonication of 13 s each; kept below 6°C by chilling in an ice-ethanol bath), and clarified by centrifugation (Fiberlite F21S-8x50y rotor; 18,000 rpm; 30 min). The soluble lysate supernatant fraction was adjusted to a final concentration of 20 mM imidazole and loaded onto a 0.5 mL Ni-NTA Superflow (Qiagen) column that was previously equilibrated with 2.5 mL Buffer E [40 mM potassium phosphate, pH 7.6, 20 mM imidazole, 500 mM NaCl, 10% (v/v) glycerol, 10 mM 2-mercaptoethanol, 0.5 mM PMSF], washed with 4 mL of Buffer E, pre-eluted with 360 µL Buffer E containing 200 mM imidazole, and eluted sequentially with 720 µL, 360 µL, and 220 µL of Buffer E containing 200 mM imidazole. This yielded 19.9 µM, 9.4 µM, and 3.5 µM hNDF, respectively, as assayed by SDS polyacrylamide gel electrophoresis with a BSA standard curve. The eluted fractions were frozen in liquid nitrogen and stored at −80°C. Next, 100 µL of Buffer TEG [10 mM Tris-HCl, pH 8.0, 1 mM EDTA, 0.01% (v/v) Nonidet P-40, 10% (v/v) glycerol, 5 mM 2-mercaptoethanol, 1 µg/mL leupeptin, 1 µg/mL pepstatin, 0.5 mM PMSF] was added to 400 µL of the 19.9 µM Ni-NTA-purification fraction and loaded onto a 300 µL anti-FLAG M2 agarose (Sigma-Aldrich) column that was pre-equilibrated with Buffer TEG containing 400 mM NaCl. The column was washed with 1.8 mL buffer TEG containing 200 mM NaCl, pre-eluted with 260 µL of Buffer TEG containing 200 mM NaCl and 500 µg/mL 3XFLAG peptide (ApexBio Technology), and eluted with 400 µL, 200 µL, and 150 µL of Buffer TEG containing 200 mM NaCl and 500 µg/mL 3XFLAG peptide. This yielded 4.5 µM, 4.4 µM, and 4.2 µM hNDF, respectively, as assayed by SDS polyacrylamide gel electrophoresis with a BSA standard curve. The purified His6-hNDF-FLAG samples were frozen in liquid nitrogen and stored at −80°C. The purified His6-hNDF-FLAG protein is shown in Supplemental Fig. S3A.

Purification of His6-yPdp3-FLAG protein

The *E. coli* codon-optimized cDNA sequence of *Saccharomyces cerevisiae* strain S288C *PDP3* (Integrated DNA Technologies; San Diego, CA) was inserted as a BspHI-XhoI fragment into pET21b-nHis6-cFLAG, which is pET21b-His6-Nco (Kassavetis et al, 1998) that was modified to

contain a C-terminal FLAG tag (LEDYKDDDDK) downstream of the XhoI site. Expression and purification of yPdp3 protein from 1 g (wet mass) of cells closely followed that of His6-hNDF-FLAG (as above) with minor changes to the Ni-NTA and anti-FLAG M2 agarose elution volumes. The Ni-NTA column was pre-eluted with 400 µL Buffer E containing 200 mM imidazole, and eluted sequentially with 700 µL, 400 µL, and 300 µL of Buffer E containing 200 mM imidazole. This yielded 166 µM, 34.7 µM, and 12.3 µM yPDP3, respectively. The M2 agarose column was pre-eluted with 250 µL of Buffer TEG containing 200 mM NaCl and 400 µg/mL 3XFLAG peptide and eluted sequentially with 500 µL, 300 µL, and 200 µL of the same buffer. This yielded 7.8 µM, 9.7 µM, and 3.7 µM yPDP3, respectively. The purified His6-yPdp3-FLAG protein is shown in Supplemental Fig. S3A.

In vitro transcription assays with calf thymus DNA

The non-specific Pol II transcription assays were carried out by using methodology similar to that described and discussed by Reinberg and Roeder (1987). Calf thymus DNA (Sigma-Aldrich; D1501; 100 mg) was dissolved in TE (10 mL) by nutation for 3 h at 4 °C, and 1 mL of the soluble material (~0.8 mg/mL) was extracted three times with phenol-chloroform-isoamyl alcohol (25:24:1, v/v/v), and precipitated with ethanol. The pellet was washed twice with 75% ethanol, dried, and dissolved in TE to a final concentration of 1.0 mg/mL. Yeast RNA polymerase II (Pol II) was diluted in 1X Transcription Buffer [20 mM Tris-HCl, pH 7.5, 5 mM $MgCl_2$, 40 mM KCl, 10 mM DTT] containing 10% (v/v) glycerol, 100 µg/mL BSA (Sigma-Aldrich; 10711454001; manufactured by Roche), and 0.5 mM PMSF. His6-dNDF was diluted in its Elution Buffer [10 mM Tris-HCl, pH 7.5, 0.2% (v/v) Nonidet P-40 (Pierce), 0.2 M NaCl, 10% (v/v) glycerol, 250 mM imidazole, and 5 mM 2-mercaptoethanol]. His6-hNDF-FLAG and His6-yPdp3-FLAG were diluted in Buffer TEG containing 200 mM NaCl and 100 µg/mL BSA. *S. cerevisiae* TFIIS (131-309) (Awrey et al. 1998; Olmsted et al. 1998) was diluted in 20 mM Tris-HCl, pH 7.5, 40 mM KCl, 10 mM dithiothreitol, 20 µM ZnSO4 and 100 µg/ml BSA. In each set of reactions,

each tube contained the equivalent combined volume of each factor and its corresponding diluent to maintain the identical composition of the buffer medium.

The standard conditions for transcription of calf thymus DNA were as follows. Reaction mixtures (20 µL final volume) were assembled with 9 µL of TE' [10 mM Tris-HCl, pH 8.0, 0.1 mM EDTA]; 2 µL of 10X Transcription Buffer; 1 µL of 10 mM each of ATP, UTP, GTP; 2 µL of 1 mg/mL calf thymus DNA; 2 µL of 75 nM Pol II or its diluent; and 2 µL of 1 µM hNDF, 1 µM yPdp3, or 3 µM dNDF or their respective diluents. This mixture was incubated for 10 min (or 15 min; the same time for each reaction in a set of reactions) at 30°C followed by the addition of 2 µL of 1 mM [α-^{32}P]CTP (700-1000 cpm/pmol) for an additional 30 min at 30°C. Reactions were stopped by spotting onto 2.4 cm DE81 filter disks (Whatman). The disks were allowed to dry for approximately 10 min and then placed in a beaker containing 100 mL of 0.35 M Na_2HPO_4 for 5 min with occasional swirling. The phosphate buffer was exchanged 6 or 7 additional times, followed by two washes with 100 mL H_2O and one wash with 100% ethanol. The filters were air-dried for >15 min prior to scintillation counting. In Fig. S1B and S3C, 2 µL of H_2O or 0.5 mg/mL α-amanitin replaced 2 µL of TE'. In Figs. S1C and S1D, Pol II was serially diluted in its diluent to achieve the final concentration shown in the figures. In Figs. 1A, 1B, S3B, S3D, and S7, hNDF, dNDF, yPdp3, and TFIIS were serially diluted in their respective diluents to achieve the final concentrations shown in the figures. In Figs. 1C and 1D, transcription was allowed to proceed for 2 to 15 min following the addition of 1 mM [α-^{32}P]CTP, as indicated in the figures.

Transcription elongation assays

In the transcription elongation assays, we assembled functional transcription elongation complexes with purified Pol II by using the method that was developed by Kashlev and colleagues (Sidorenkov et al. 1998; Kireeva et al. 2000; Komissarova et al. 2003). In this method, a short RNA primer is hybridized to the template DNA strand (TS), and then purified RNA polymerase II is added to the RNA:DNA hybrid to reconstitute the catalytically active elongation complex. Next, the complementary non-template DNA strand (NTS) is annealed to

give the elongation complex with both strands of DNA. With this method, the stepwise assembly of an elongation complex starting with an 8 or 9 bp RNA:DNA hybrid has all of the features of a normal elongation complex – resistance to treatment with 1 M KCl as well as maintenance and movement of the transcription bubble upon addition of NTPs with concomitant reannealing of upstream DNA as measured by $KMnO_4$ footprinting (Kireeva et al. 2000). For these reasons, the Kashlev system has been widely used to study transcriptional elongation.

In our experiments, the template strand (TS), non-template strand (NTS), RNA primer, and 5S rDNA sequences were identical to those described in Fei et al. (2018). The elongation assays were performed as in Fei et al. (2018), except that purified human Pol II (Malik and Roeder 2003) was used at a working concentration of 120 nM. Briefly, the 10 nt 5'-^{32}P-labeled primer RNA was annealed to an equimolar amount of template strand (TS) DNA. Purified Pol II was then added to the RNA-TS complex, and the components were incubated at 30˚C for 10 min. Next, the 5'-biotin-labeled non-template strand (NTS) was added and incubated at 30˚C for 15 min to form the elongation complex, which was then immobilized onto Dynabeads MyOne Streptavidin C1 magnetic beads (Invitrogen). The beads were washed, and the elongation complexes were ligated to the downstream DNA fragments (either 5S rDNA or *FXN* gene fragment). The beads were then aliquoted into tubes for the individual reactions. hNDF or the corresponding buffer (as a negative control) was added to each tube. Then, transcription elongation was initiated by the addition of rNTPs, and the reactions were allowed to proceed at 22˚C for the indicated times. The reactions were terminated, and the samples were analyzed by denaturing 8% polyacrylamide-urea gel electrophoresis. The gel images were collected on a GE Typhoon imager (GE Healthcare). Additional details of the methodology are provided in Fei et al. (2018).

The *FXN* trinucleotide repeat sequences were PCR-amplified from the pFXN-GAA plasmid containing ~400 GAA trinucleotide repeats by using the following primers (forward: 5'-CATTAGGGCACTGGGATTGGTTGCCTGTGCTTAAAAGTTAG-3', TspRI site is underlined; reverse: 5'-GATCTAAGGACCATCATGGCCACACTTGCC-3'). The PCR products were

digested with the TspRI restriction enzyme (NEB), gel purified, and ligated to the Pol II elongation complex. The pause rescue experiments were performed as previously described (Xu et al. 2017). The oligonucleotides that were used are described in the main text.

Co-immunoprecipitation analyses

HeLa cells expressing FLAG-hNDF-GFP were collected and lysed in NETN buffer [20 mM Tris-HCl, pH 8.0, 100 mM NaCl, 1 mM EDTA, 1 mM $MgCl_2$, 0.5% (v/v) Nonidet P-40, and Mini Protease Inhibitor (MilliporeSigma;11836153001)] for 30 min at 4 °C. Each lysate was subjected to 3 cycles of sonication of 10 s each, and then clarified by microcentrifugation (15,000 × *g*, 10 min, 4 °C). The supernatant was incubated with FLAG M2 agarose (Sigma) for 2 h at 4 °C on a nutator. The beads were then washed three times with ice-cold NETN buffer, resuspended in 1x SDS sample buffer, and analyzed by western blotting with antibodies against Pol II (Santa Cruz Biotechnology; sc-9001) or FLAG. For endogenous hNDF immunoprecipitation, HeLa cells extracts were incubated with anti-hNDF antibodies (anti-hNDF serum #6; Fei et al. 2018) for 4 h and another 4 h with protein A beads (Invitrogen) at 4 °C on a nutator. After three washes with ice-cold NETN buffer, immunoprecipitates were released from the beads by boiling in 1× SDS sample buffer and resolved by SDS polyacrylamide gel electrophoresis. Proteins were transferred to a polyvinylidene fluoride (PVDF) membrane (Millipore). The membrane was blocked by incubation with a 1x TBST buffer containing 5% (w/v) bovine serum albumin (Sigma) for 1 h at room temperature. The membrane was then probed with antibodies against Pol II (Santa Cruz Biotechnology; sc-9001) or hNDF (anti-hNDF serum #6; Fei et al. 2018).

Bru-seq experiments

For each Bru-seq (Paulsen et al. 2013) experiment, about 1.5 x 10^7 wild-type and NDF knockout (KO) HeLa cells (Fei et al. 2018) were seeded and maintained in a 15 cm dish about 16 h before the experiment. Cell culture media were then replaced with 15 mL fresh complete media containing 2 mM 5-bromouridine (MilliporeSigma, 850187). Cells were further incubated for 10

min in the incubator (37 °C, 5% CO_2) to let the 5-bromouridine incorporate into the nascent RNA. To stop the reaction, cells on the culture plate were quickly washed once with 10 mL 1x PBS. After complete removal of PBS, 3 mL TRIzol LS (ThermoFisher, Invitrogen, 10296010) was added directly to the cells. RNA was purified by using a standard isopropanol precipitation protocol. The 5-bromouridine-labeled RNAs were isolated as described (Paulsen et al. 2013). Sequencing libraries were prepared with the NEBNext Small RNA Library Prep Set for Illumina (NEB, E7330S) and sequenced at the UCSD NGS core facility. The data were mapped to the hg19 genome with Bowtie2 (Langmead and Salzberg 2012) and analyzed by using HOMER (Heinz et al. 2010). Reads in gene bodies (TSS to TTS) were counted, normalized to 10^7 reads, and analyzed by using JMP Pro 15 (SAS Institute Inc).

NDF knockout and knockout rescue in SW480 cells

Human colorectal adenocarcinoma SW480 cells were a generous gift from Dr. Shannon Lauberth (Northwestern University). The SW480 cells were cultured with Dulbecco's modified Eagle's medium (DMEM) containing 10% (v/v) fetal bovine serum (FBS; Gibco), 100 units/mL penicillin, and 0.1 mg/mL streptomycin. Cells were maintained in a humidified incubator atmosphere at 37 °C with 5% CO_2. hNDF CRISPR-Cas9 knockout (KO) SW480 cells were generated by using a guide RNA targeting the hNDF genomic sequence (5'-AACTCGGCCGATATCCTCCT-3'). This sequence was cloned into the Cas9-GFP PX458 vector, and the resulting plasmid was transfected into SW480 cells by using polyethylenimine (PEI) (Polysciences, Inc.; Warrington, PA) according to the recommendations of the manufacturer. GFP-positive single cell clones were cultured and used in this study. NDF knockouts were confirmed by western blot analysis with anti-hNDF antibodies. For knockout rescue experiments, CRISPR-resistant hNDF cDNA was generated by mutating the nucleotides shown in blue (5'-AACTCGGCCGATACCCACCA-3'). CRISPR-resistant hNDF constructs were then cloned into pHR-IRES-puro vector (gift from Dr. Enfu Hui's lab, UCSD). Lentiviruses carrying untagged hNDF cDNA were generated by co-transfecting pHR-IRES-puro-hNDF,

psPAX2, and pMD2.G into HEK293T cells. At 48 hours post transfection, HEK293T cell media containing lentiviruses were collected and used to infect hNDF knockout (KO) SW480 cells. After infection, the NDF rescue cells (KO + NDF rescue) were selected for puromycin resistance (0.5 μg/ml). Western blots with anti-hNDF antibody were performed to confirm the successful expression of hNDF in the KO + NDF rescue SW480 cells.

Supplemental References

Awrey DE, Shimasaki N, Koth C, Weilbaecher R, Olmsted V, Kazanis S, Shan X, Arellano J, Arrowsmith CH, Kane CM, et al. 1998. Yeast transcript elongation factor (TFIIS), structure and function. II: RNA polymerase binding, transcript cleavage, and read-through. *J Biol Chem* **273:** 22595-22605.

Fei J, Ishii H, Hoeksema MA, Meitinger F, Kassavetis GA, Glass CK, Ren B, Kadonaga JT. 2018. NDF, a nucleosome-destabilizing factor that facilitates transcription through nucleosomes. *Genes Dev* **32:** 682-694.

Gilbert TM, McDaniel SL, Byrum SD, Cades JA, Dancy BC, Wade H, Tackett AJ, Strahl BD, Taverna SD. 2014. A PWWP domain-containing protein targets the NuA3 acetyltransferase complex via histone H3 lysine 36 trimethylation to coordinate transcriptional elongation at coding regions. *Mol Cell Proteomics* **13:** 2883-2895.

Heinz S, Benner C, Spann N, Bertolino E, Lin YC, Laslo P, Cheng JX, Murre C, Singh H, Glass CK. 2010. Simple combinations of lineage-determining transcription factors prime cis-regulatory elements required for macrophage and B cell identities. *Mol Cell* **38:** 576–589.

Kaplan CD, Larsson KM, Kornberg RD. 2008. The RNA polymerase II trigger loop functions in substrate selection and is directly targeted by alpha-amanitin. *Mol Cell* **30:** 547-556.

Kassavetis GA, Kumar A, Ramirez E, Geiduschek EP 1998. Functional and structural organization of Brf, the TFIIB-related component of the RNA polymerase III transcription initiation complex. *Mol Cell Biol* **18:** 5587-5599.

Kireeva ML, Komissarova N, Waugh DS, Kashlev M. 2000. The 8-nucleotide-long RNA:DNA hybrid is a primary stability determinant of the RNA polymerase II elongation complex. *J Biol Chem* **275:** 6530-6536.

Komissarova N, Kireeva ML, Becker J, Sidorenkov I, Kashlev M. 2003. Engineering of elongation complexes of bacterial and yeast RNA polymerases. *Methods Enzymol* **371:** 233-251.

Langmead B, Salzberg SL. 2012. Fast gapped-read alignment with Bowtie 2. *Nat Methods* **9:** 357–359.

Malik S, Roeder RG. 2003. Isolation and functional characterization of the TRAP/mediator complex. *Methods Enzymol* **364:** 257-284.

Olmsted VK, Awrey DE, Koth C, Shan X, Morin PE, Kazanis S, Edwards AM, Arrowsmith CH. 1998. Yeast transcript elongation factor (TFIIS), structure and function. I: NMR structural analysis of the minimal transcriptionally active region. *J Biol Chem* **273:** 22589-22594.

Paulsen MT, Veloso A, Prasad J, Bedi K, Ljungman EA, Tsan YC, Chang CW, Tarrier B, Washburn JG, Lyons R, et al. 2013. Coordinated regulation of synthesis and stability of RNA during the acute TNF-induced proinflammatory response. *Proc Natl Acad Sci* **110:** 2240-2245.

Reinberg D, Roeder RG. 1987. Factors involved in specific transcription by mammalian RNA polymerase II. Transcription factor IIS stimulates elongation of RNA chains. *J Biol Chem* **262:** 3331-3337.

Sidorenkov I, Komissarova N, Kashlev M. 1998. Crucial role of the RNA:DNA hybrid in the processivity of transcription. *Mol Cell* **2:** 55-64.

Xu J, Lahiri I, Wang W, Wier A, Cianfrocco MA, Chong J, Hare AA, Dervan PB, DiMaio F, Leschziner AE, et al. 2017. Structural basis for the initiation of eukaryotic transcription-coupled DNA repair. *Nature* **551:** 653-657.

Supplemental Table S1. Raw data for the calf thymus DNA transcription assays

Supplemental Table S1A (data for Fig. 1A)

Condition	CPM rep 1	CPM rep 2	CPM rep 3	Mean ±SD	CPM−(a) rep 1	CPM−(a) rep 2	CPM−(a) rep 3	Mean−(a) ±SD
Background (no protein)	127	132	126	128 ±3 (a)	−1	4	−2	0 ±4
Pol II only	767	792	942	834 ±77	639	664	814	705 ±77 (b)
6.25 nM hNDF+Pol II	1091	1113	1106	1103 ±9	963	985	978	975 ±10
12.5 nM hNDF+Pol II	1149	1213	1153	1172 ±29	1021	1085	1025	1043 ±29
25 nM hNDF+Pol II	1487	1390	1668	1515 ±115	1359	1262	1540	1387 ±115
50 nM hNDF+Pol II	2330	2284	2235	2283 ±39	2202	2156	2107	2155 ±39
100 nM hNDF+Pol II	2907	2702	2738	2782 ±89	2779	2574	2610	2654 ±89
200 nM hNDF+Pol II	2735	2642	2523	2633 ±87	2607	2514	2395	2505 ±87

Pol II: Yeast RNA polymerase II. When included, Pol II was used at a final concentration of 7.5 nM.
hNDF: Human NDF
SD: Standard deviation
CPM: Counts per minute
rep: Replicate number
(a) Mean background CPM
(b) This value was set to 1.0 for normalization in Fig. 1A. Specifically, the values in the rightmost four columns in the table above were divided by 705 in the graph shown in Fig. 1A.

Supplemental Table S1B (data for Fig. 1B)

Condition	CPM rep 1	CPM rep 2	CPM rep 3	Mean ±SD	CPM−(a) rep 1	CPM−(a) rep 2	CPM−(a) rep 3	Mean−(a) ±SD
Background (no protein)	154	135	179	156 ±18 (a)	−2	−21	23	0 ±25
Pol II only	445	447	484	459 ±18	289	291	328	303 ±25 (b)
25 nM dNDF+Pol II	929	867	877	891 ±27	773	711	721	735 ±33
50 nM dNDF+Pol II	1327	1338	1280	1315 ±25	1171	1182	1124	1159 ±31
100 nM dNDF+Pol II	1648	1618	1579	1615 ±28	1492	1462	1423	1459 ±34
200 nM dNDF+Pol II	1829	1896	2006	1910 ±72	1673	1740	1850	1754 ±75
400 nM dNDF+Pol II	1979	2040	1912	1977 ±52	1823	1884	1756	1821 ±55

Pol II: Yeast RNA polymerase II. When included, Pol II was used at a final concentration of 7.5 nM.
dNDF: *Drosophila* NDF
SD: Standard deviation
CPM: Counts per minute
rep: Replicate number
(a) Mean background CPM
(b) This value was set to 1.0 for normalization in Fig. 1B. Specifically, the values in the rightmost four columns in the table above were divided by 303 in the graph shown in Fig. 1B.

Supplemental Table S1C (data for Fig. 1C and Fig. S1B)

Time (min)	CPM rep 1	CPM rep 2	CPM rep 3	Mean ±SD	CPM−(c) rep 1 (d)	CPM−(c) rep 2 (d)	CPM−(c) rep 3 (d)	Mean−(c) ±SD (d)
Time course with 7.5 nM Pol II								
0 (a,b)	204	215	205	208 ±5 (c)	−4	7	−3	0 ±7
2	423	412	427	421 ±6	215	204	219	213 ±8
5	421	466	441	443 ±18	213	258	233	235 ±19
8	480	481	510	490 ±14	272	273	302	282 ±15
11	559	516	541	539 ±18	351	308	333	331 ±18
15 (b)	623	546	584	584 ±31	415	338	376	376 ±32
Time course with 7.5 nM Pol II and 100 nM hNDF								
0 (a,b)	199	221	221	214 ±10	−9	13	13	6 ±12
2	1108	1063	920	1030 ±80	900	855	712	822 ±80
5	1552	1554	1382	1496 81±	1344	1346	1174	1288 ±81
8	2007	1938	1649	1865 ±155	1799	1730	1441	1657 ±155
11	2458	2385	2010	2284 ±196	2250	2177	1802	2076 ±196
15 (b)	3009	2861	2513	2794 ±208	2801	2653	2305	2586 ±208

Pol II: Yeast RNA polymerase II
hNDF: Human NDF
SD: Standard deviation
CPM: Counts per minute
rep: Replicate number
(a) The 0 min time points lacked Pol II and were incubated for 15 min.
(b). The numbers in blue type were also used in the hNDF panel of Fig. S1B, in which the values were divided by 376 in the y-axis of the plot.
(c) Mean background CPM
(d) The values in the rightmost four columns in the table above were divided by 500 in the graph shown in Fig. 1C.

Supplemental Table S1D (data for Fig. 1D and Fig. S1B)

Time (min)	CPM rep1	CPM rep2	CPM rep3	Mean ± SD	CPM−(c) rep1 (d)	CPM−(c) rep2 (d)	CPM−(c) rep3 (d)	Mean−(c) ± SD (d)
Time course with 7.5 nM Pol II								
0 (a,b)	169	158	139	155 ±12 (c)	14	3	(16)	0 ±18
2	519	550	540	536 ±13	364	395	385	381 ±18
5	712	648	644	668 ±31	557	493	489	513 ±34
8	843	786	758	796 ±35	688	631	603	640 ±37
11	959	929	895	928 ±26	804	774	740	772 ±29
15 (b)	1124	1026	1014	1055 ±49	969	871	859	899 ±51
Time course with 7.5 nM Pol II and 300 nM dNDF								
0 (a,b)	151	137	147	145 ±6	−4	−18	−8	−10 ±14
2	1424	1380	1225	1343 ±85	1269	1225	1070	1188 ±86
5	2194	2096	1945	2078 ±102	2039	1941	1790	1923 ±103
8	2899	2768	2567	2745 ±137	2744	2613	2412	2589 ±137
11	3370	3489	3092	3317 ±166	3215	3334	2937	3162 ±167
15 (b)	4323	4146	3943	4137 ±155	4168	3991	3788	3982 ±156

Pol II: Yeast RNA polymerase II
dNDF: *Drosophila* NDF
SD: Standard deviation
CPM: Counts per minute
rep: Replicate number
(a) The 0 min time points lacked Pol II and were incubated for 15 min.
(b). The numbers in blue type were also used in the dNDF panel of Fig. S1B, in which the values were divided by 899 in the y-axis of the plot.
(c) Mean background CPM
(d) The values in the rightmost four columns in the table above were divided by 1000 in the graph shown in Fig. 1D.

Supplemental Table S1E (data for α-amanitin graph in Fig. S1B)

Components	CPM rep1	CPM rep2	CPM rep3	Mean ±SD	CPM−(a) rep1 (b)	CPM−(a) rep2 (b)	CPM−(a) rep3 (b)	Mean−(a) ±SD (b)
hNDF	181	166	172	173 ±6 (a)	8	−7	−1	0 ±9
Pol II	1217	1172	1188	1192 ±19	1044	999	1015	1019 ±20
hNDF+Pol II	3418	3428	3322	3389 ±48	3245	3255	3149	3216 ±48
hNDF+Pol II+α-amanitin	205	187	197	196 ±7	32	14	24	23 ±10

hNDF: Human NDF. When included, hNDF was used at a final concentration of 100 nM.
Pol II: Yeast RNA polymerase II. When included, Pol II was used at a final concentration of 7.5 nM.
α-amanitin: When included, α-amanitin was used at a final concentration of 50 µg/mL.
CPM: Counts per minute
rep: Replicate number
SD: Standard deviation
(a) Mean background CPM
(b) The values in the rightmost four columns in the table above were divided by 1000 in the graph shown in Fig. S1B.

Supplemental Table S1F (data for Fig. S1C)

Pol II (nM)	CPM rep1	CPM rep2	CPM rep3	Mean ±SD	CPM−(a) rep1 (b)	CPM−(a) rep2 (b)	CPM−(a) rep3 (b)	Mean−(a) ±SD (b)
Pol II titration without hNDF								
0	148	128	141	139 ±8 (a)	9	−11	2	0 ±12
2.5	203	155	215	191 ±26	64	16	76	52 ±27
5	284	249	464	332 ±94	145	110	325	193 ±95
10	1668	1533	1633	1611 ±57	1529	1394	1494	1472 ±58
20	6260	5359	5897	5838 ±370	6121	5220	5758	5700 ±370
Pol II titration with 100 nM hNDF								
0	132	147	155	145 ±10	−7	8	16	6 ±13
2.5	882	976	923	927 ±38	743	837	784	788 ±39
5	1795	1867	1782	1815 ±37	1656	1728	1643	1676 ±38
10	3681	3677	3500	3619 ±84	3542	3538	3361	3480 ±85
20	7592	7366	7066	7341 ±215	7453	7227	6927	7202 ±216

Pol II: Yeast RNA polymerase II. The final concentrations of Pol II are indicated in nM.
hNDF: Human NDF. When included, hNDF was used at a final concentration of 100 nM.
CPM: Counts per minute
rep: Replicate number
SD: Standard deviation
(a) Mean background CPM
(b) The values in the rightmost four columns in the table above were divided by 2000 in the graph shown in Fig. S1C.

Supplemental Table S1G (data for Fig. S1D)

Pol II (nM)	CPM rep1	CPM rep2	CPM rep3	Mean ±SD	CPM−(a) rep1 (b)	CPM−(a) rep2 (b)	CPM−(a) rep3 (b)	Mean−(a) ±SD (b)
Pol II titration without dNDF								
0	149	162	144	152 ±8 (a)	−3	10	−8	0 ±11
2.5	253	281	254	263 ±13	101	129	102	111 ±15
5	614	648	709	657 ±39	462	496	557	505 ±40
10	2628	2761	2922	2770 ±120	2476	2609	2770	2619 ±120
20	7837	8030	8202	8023 ±149	7685	7878	8050	7871 ±149
Pol II titration with 300 nM dNDF								
0	166	178	184	176 ±7	14	26	32	24 ±11
2.5	1298	1329	1244	1290 ±35	1146	1177	1092	1139 ±36
5	2746	2263	2647	2552 ±208	2594	2111	2495	2400 ±208
10	5073	5303	5232	5203 ±96	4921	5151	5080	5051 ±96
20	8867	9605	9481	9318 ±323	8715	9453	9329	9166 ±323

Pol II: Yeast RNA polymerase II. The final concentrations of Pol II are indicated in nM.
dNDF: *Drosophila* NDF. When included, dNDF was used at a final concentration of 300 nM.
CPM: Counts per minute
rep: Replicate number
SD: Standard deviation
(a) Mean background CPM
(b) The values in the rightmost four columns in the table above were divided by 2000 in the graph shown in Fig. S1D.

Supplemental Table S1H (data for Fig. S3B)

Condition	CPM rep 1	CPM rep 2	CPM rep 3	Mean ±SD	CPM−(a) rep 1	CPM−(a) rep 2	CPM−(a) rep 3	Mean−(a) ±SD
Background (no protein)	91	73	67	77 ±10 (a)	14	−4	−10	0 ±14
Pol II only	657	560	608	608 ±40	580	483	531	531 ±41 (b)
6.25 nM yPdp3 + Pol II	811	682	765	753 ±53	734	605	688	676 ±54
12.5 nM yPdp3 + Pol II	931	997	988	972 ±29	854	920	911	895 ±31
25 nM yPdp3 + Pol II	2300	2251	2130	2227 ±71	2223	2174	2053	2150 ±72
50 nM yPdp3 + Pol II	2632	2881	2835	2783 ±108	2555	2804	2758	2706 ±109
100 nM yPdp3 + Pol II	2786	2984	3045	2938 ±111	2709	2907	2968	2861 ±111
200 nM yPdp3 + Pol II	2946	2665	2535	2715 ±172	2869	2588	2458	2638 ±172

Pol II: Yeast RNA polymerase II. When included, Pol II was used at a final concentration of 7.5 nM.
yPdp3: *S. cerevisiae* Pdp3 protein
SD: Standard deviation
CPM: Counts per minute
rep: Replicate number
(a) Mean background CPM
(b) This value was set to 1.0 for normalization in Fig. S3B. Specifically, the values in the rightmost four columns in the table above were divided by 531 in the graph shown in Fig. S3B.

Supplemental Table S1l (data for Fig. S3C)

Components	CPM rep1	CPM rep2	CPM rep3	Mean ±SD	CPM−(a) rep1	CPM−(a) rep2	CPM−(a) rep3	Mean−(a) ±SD
Background (no protein)	135	117	132	128 ±8 (a)	7	−11	4	0 ±11
yPdp3 only	116	108	123	116 ±6	−12	−20	−5	−12 ±10
Pol II only	1122	1034	1055	10706 ±38	994	906	927	942 ±38 (b)
yPdp3 + Pol II	2684	2723	3104	2837 ±189	2556	2595	2976	2709 ±190
yPdp3 + Pol II + α-amanitin	159	129	122	137 ±16	31	1	−6	9 ±18

Pol II: Yeast RNA polymerase II. When included, Pol II was used at a final concentration of 7.5 nM.
yPdp3: *S. cerevisiae* Pdp3 protein. When included, yPdp3 was used at a final concentration of 100 nM.
α-amanitin: When included, α-amanitin was used at a final concentration of 50 µg/ml.
SD: Standard deviation
CPM: Counts per minute
rep: Replicate number
(a) Mean background CPM
(b) This value was set to 1.0 for normalization in Fig. S3C. Specifically, the values in the rightmost four columns in the table above were divided by 942 in the graph shown in Fig. S3C.

Supplemental Table S1J (data for Fig. S3D)

Condition	CPM rep 1	CPM rep 2	CPM rep 3	Mean±SD	CPM−(a) rep 1	CPM−(a) rep 2	CPM−(a) rep 3	Mean−(a) ±SD
Background (no protein)	(c)	123	126	124±2 (a)	(c)	−2	2	0±2
Pol II only	984	969	982	978±7	860	844	858	854±7 (b)
50 nM hNDF+Pol II	2484	2330	2498	2437±76	2360	2206	2374	2313±76
100 nM hNDF+Pol II	2778	2442	2598	2606±137	2654	2318	2474	2482±137
200 nM hNDF+Pol II	2701	3014	3239	2985±221	2576	2890	3114	2860±221
50 nM yPdp3+Pol II	3009	2710	2817	2845±124	2884	2586	2692	2721±124
100 nM yPdp3+Pol II	3224	2829	2995	3016±162	3100	2704	2870	2892±162
200 nM yPdp3+Pol II	2821	2750	2529	2700±124	2696	2626	2404	2576±124
50nM hNDF + 50 nM yPdp3 + Pol II	2362	2634	2306	2434±143	2238	2510	2182	2310±143
100nM hNDF + 100 nM yPdp3+Pol II	2174	1848	2874	2299±428	2050	1724	2750	2174±428

Pol II: Yeast RNA polymerase II. When included, Pol II was used at a final concentration of 7.5 nM.
hNDF: Human NDF
yPdp3: *S. cerevisiae* Pdp3 protein
SD: Standard deviation
CPM: Counts per minute
rep: Replicate number
(a) Mean background CPM
(b) This value was set to 1.0 for normalization in Fig. S3D. Specifically, the values in the rightmost four columns in the table above were divided by 854 in the graph shown in Fig. S3D.
(c) Lost sample

Supplemental Table S1K (data for Fig. S7)

Condition	CPM rep 1	CPM rep 2	CPM rep 3	Mean±SD	CPM−(a) rep 1	CPM−(a) rep 2	CPM−(a) rep 3	Mean−(a) ±SD
Background (no protein)	140	146	137	141±4 (a)	−1	5	−4	0 ± 4
100 nM TFIIS only	136	129	101	122±15	−5	−12	−40	−19 ±16
Pol II only	1202	1193	1161	1185±18	1061	1052	1020	1044 ±18 (b)
50 nM hNDF+Pol II	2941	3156	3261	3119±133	2800	3015	3120	2978 ±133
100 nM hNDF+Pol II	3623	3561	3411	3532±89	3482	3420	3270	3391 ±89
200 nM hNDF+Pol II	3158	3018	3213	3130±82	3017	2877	3072	2989 ±82
25 nM TFIIS+Pol II	2049	2121	2217	2129±69	1908	1980	2076	1988 ±69
50 nM TFIIS+Pol II	2269	2312	2173	2251±58	2128	2171	2032	2110 ±58
100 nM TFIIS+Pol II	2232	2160	(c)	2196±36	2091	2019	(c)	2055 ±36
50nM hNDF+25 nM TFIIS+Pol II	5565	5861	5846	5757±136	5424	5720	5705	5616 ±136
100nM hNDF+50 nM TFIIS+Pol II	6659	5922	4628	5736±839	6518	5781	4487	5595 ±839

Pol II: Yeast RNA polymerase II. When included, Pol II was used at a final concentration of 7.5 nM.
TFIIS: *S. cerevisiae* TFIIS (131-309), which has complete transcriptional activity of full-length TFIIS (Olmstead et al. 1998).
hNDF: Human NDF
SD: Standard deviation
CPM: Counts per minute
rep: Replicate number
(a) Mean background CPM
(b) This value was set to 1.0 for normalization in Fig. S7. Specifically, the values in the rightmost four columns in the table above were divided by 1044 in the graph shown in Fig. S7.
(c) Lost sample